SLAC-PUB-16520

HADRONIC WAVEFUNCTIONS AND HIGH MOMENTUM TRANSFER INTERACTIONS IN QUANTUM CHROMODYNAMICS

Stanley J. Brodsky
Stanford Linear Accelerator Center, Stanford, CA 94305, USA

Tao Huang
Stanford Linear Accelerator Center, Stanford, CA 94305, USA
and Institute of High Energy Physics, Beijing
People's Republic of China

G. Peter Lepage
Laboratory of Nuclear Studies
Cornell University, Ithaca, New York 14853, USA

I. INTRODUCTION

Quantum Chromodynamics is a renormalizable non-Abelian gauge field theory of quarks and gluons, based on the principle of exact local SU(3)-color symmetry.[1] From the experimental standpoint, there is now impressive evidence[2] that QCD is a viable theory of hadronic phenomena. The most important phenomenological evidence for QCD comes from inelastic lepton scattering, e^+e^- annihilation processes, and those high momentum transfer exclusive and inclusive reactions where the structure of perturbative quark and gluon subprocesses can be studied in relative isolation from the bound state dynamics of the hadrons. From the theoretical standpoint, the elegant structure of QCD makes it appear almost compelling as a fundamental theory of hadronic phenomena, even though many crucial questions concerning quark and gluon confinement, and the effects of non-perturbative phenomena remain unanswered.[3]

A critical feature of QCD is asymptotic freedom,[4] i.e., the logarithmic decrease of the effective quark and gluon coupling constant $\alpha_s(Q^2)$ with momentum transfer which implies that the strong interactions become weak, and even calculable in perturbative theory at short distance. The fact that the annihilation ratio

$$R_{e^+e^-}(s) = \frac{\sigma(e^+e^- \to \text{hadrons})}{\sigma(e^+e^- \to \mu^+\mu^-)} \tag{1.1}$$

This material is based upon work supported by the U.S. Department of Energy, Office of Science, Office of Basic Energy Sciences, under Contract No. DE-AC02-76SF00515 and HEP.

is empirically[5] close to the zeroth order QCD prediction $R^o = 3 \sum_q e_q^2$ for energies above the heavy quark thresholds is a crucial check of asymptotic freedom and the color, charge, and spin assignments of the quark quanta in QCD. Critical features of QCD are also confirmed by the observed logarithmic breaking of scale-invariance in deep inelastic lepton-scattering[2] and the measurements of two-jet and three-jet structure of e^+e^- annihilation final states.[5] The recent observations of jet structure[6] in two-photon reactions (consistent with $\gamma\gamma \to q\bar{q}$ subprocesses), and measurements[7] of the photon structure function also provide fundamental checks of predictions which are essentially unique to QCD. However, despite these successes, there is no direct experimental evidence for (near) scale-invariant quark-quark, quark-gluon, or gluon-gluon scattering amplitudes as predicted by QCD; the cross section for large transverse momentum hadron production in hadron-hadron collisions appears to reflect much more complicated dynamical mechanisms. On the other hand, as we discuss in Section IV, the fact that the proton form factor $G_M(Q^2)$ scales as $(Q^2)^{-2}$ reflects the fact that the minimum Fock state in the nucleon contains 3 quarks, and that the internal quark-quark interactions which control the nucleon wavefunction at short distances are consistent with scale invariance.[8,9] Thus far experiments are not sufficiently sensitive to distinguish a logarithmically decreasing $\alpha_s(Q^2)$ from a constant; i.e., fixed point behavior. The sensitivity of the nucleon form factors to the form of $\alpha_s(Q^2)$ is discussed in Section VI.

Although there have been remarkable technical achievements in perturbative QCD calculations in the past few years,[1,2,10] there has also been the realization that precise and detailed comparisons with experiment require consideration of effects and phenomena not readily computable with present methods. There are, in fact, only a very few large momentum transfer processes which can be studied rigorously to all orders in perturbation theory such as $R_{e^+e^-}(s)$,[1] the meson form factors $F_M(Q^2)$[11] (and $F_{\gamma\to M}(Q^2)$), the two photon processes[12] $\gamma\gamma \to M\bar{M}$ at large momentum transfer, the photon structure function,[13] and the Q^2-evolution of the hadron structure functions. Although, in principle, these processes can be calculated to arbitrary orders in perturbation theory, in practice, there are serious complications involving the dependence of predictions made to finite order on the choice of renormalization scheme and the scale parametrization chosen for the argument of α_s.[2,13] We discuss a new method for avoiding the ambiguities in Reference 14. Aside from this, there is always the question of the radius of convergence of the perturbation expansion. Even for processes which can be calculated to arbitrary orders in α_s, there are (presently) uncalculable power-law suppressed (higher twist) contributions[15] which must be included in detailed fits to experiment, especially at the edge of phase space.[16]

In the case of jet production, QCD-based predictions based on

the elementary features of $e^+e^- \to q\bar{q}$ and $q\bar{q}g$, $\gamma\gamma \to q\bar{q}$, etc. must also take into account higher twist contributions, model-dependent non-perturbative effects intrinsic to hadron formation and decay,[5] and possibly dynamical effects due to quark confinement.[3] In the case of some exclusive processes such as the baryon form factor there are non-leading QCD contributions which are asymptotically suppressed by Sudakhov form factors.[9,10] The precise evaluation requires an all orders resumption of perturbation theory. QCD predictions for elastic hadron-hadron scattering are complicated by the presence of Landshoff[17] pinch singularity contributions which are only partially suppressed by Sudakhov form factors.[10] Despite these complications, we can still derive general properties for exclusive reactions such as hadron-helicity conservation[18] and the leading power-law behavior.[19]

An even more interesting (and perplexing) situation occurs for all inclusive high momentum transfer inclusive reactions involving hadronic initial states such as Drell-Yan massive lepton pair production, direct photon production, and large p_T hadron production. As shown in Reference 20, initial state interactions violate the usual QCD factorization theorem order by order in perturbation theory and affect the normalization and transverse momentum dependence of the inclusive cross sections. In addition, final state interactions also affect the associated multiplicity and transverse momentum dependence of the outgoing jets in deep inelastic lepton scattering reactions. A detailed report on these effects is given in Reference 20.

Perhaps the most serious complication to QCD phenomenology is the presence of higher twist subprocesses, since power-law suppressed contributions can often mimic (and thus confuse the identification) of the logarithmic modifications predicted for the leading twist contributions.[16] Examples of this for deep inelastic structure functions and fragmentation distributions are discussed in References 21 and 22 and Section V. In the case of three-jet production in e^+e^- annihilation, higher twist terms give contributions[23] $dN/dk_\perp^2 \sim (k_\perp^2)^{-2}$ for the hadron transverse momentum distribution in quark and gluon jets. These hard components can complicate the separation of the $e^+e^- \to q\bar{q}g$ and $e^+e^- \to q\bar{q}$ subprocesses. In the case of hadron production at large transverse momentum, "direct-coupled" higher twist subprocesses such as $gq \to \pi q$ actually dominate[24] the leading twist $qq \to qq \to q\pi q$ subprocess at large $x_T = 2p_T/\sqrt{s}$. Evidence for direct-coupled $\pi q \to \gamma^* q$ subprocesses in $\pi p \to \mu^+\mu^- x$ reactions is discussed in Section V and Reference 22.

Present QCD phenomenology is also incomplete in the sense that although much attention is paid to the Q^2 evolution of hadron structure functions there is no real understanding of the basic x-dependent form of the quark and gluon distribution in hadrons,

or, how to relate them to other hadronic phenomena. The relation of the $x \sim 1$ behavior of structure functions to the exclusive fixed W^2, high Q^2 domain is only roughly understood.[25] The $x \sim 0$ behavior of structure functions and the connection to the photoabsorption cross section at fixed Q^2, high ν, and nuclear shadowing phenomena is also not well understood.[26]

These lectures are part of a series presented in this volume by G.P. Lepage, G. Bodwin and myself. Our purpose is to begin to extend QCD phenomenology by taking into account both the physics of hadronic wavefunctions[27] and the effects of initial and final state interactions.[20] The work presented here on the construction and parametrization of wavefunctions in QCD was done in collaboration with Tao Huang. The work on initial state effects is presented in the chapter by G. Bodwin. Our eventual goal is to obtain a parametrization of the wavefunctions which will bridge the gap between the non-perturbative and perturbative aspects of QCD. The lack of knowledge of hadronic matrix elements is the main difficulty in computing and normalizing dynamical higher twist contributions for many processes.

In these lectures we emphasize the utility of a Fock state representation of the meson and baryon wavefunctions as a means not only to parametrize the effects of bound state dynamics in QCD phenomena, but also to interrelate exclusive, inclusive, and higher twist processes. It is particularly convenient to choose a momentum space Fock state basis[19,27]

$$\psi_n(x,\vec{k}_{\perp i},\lambda_i) \; ; \quad \sum_{i=1}^{n} x_i = 1 \; , \quad \sum_{i=1}^{n} \vec{k}_{\perp i} = 0 \; ,$$

defined at equal "time" $\tau = t+z$ on the light-cone. Here $x_i = (k^o+k^3)_i/(p^o+p^3)$, $\vec{k}_{\perp i}$, and λ_i specify the longitudinal and transverse momenta and spin projection S_z of each (on-mass-shell) quark and gluon in the n-particle Fock state ($n \geq 2$ for mesons and $n \geq 3$ for baryons). We also choose the light-cone gauge $A^+ = A^o + A^3 = 0$ so that only physical polarizations of the gluons occur. The color singlet wavefunctions are regulated so that they are finite in both the infrared and ultraviolet regimes.[28]

There are a number of reasons why this representation of hadrons in terms of the quark and gluon degrees of freedom is useful:

(1) In light-cone perturbation theory, the perturbative vacuum is also an eigenstate of the total QCD Hamiltonian on the light-cone; perturbative calculations are enormously simplified by the absence of vacuum to pair production amplitudes.

(2) All form factors, charge radii, magnetic moments, etc. have exact expressions in terms of the ψ_n.

(3) The structure functions $G_q(x,Q)$ and $G_g(x,Q)$ (and more general multiparticle distributions)which control large momentum transfer (leading and higher twist) inclusive reactions, and the distribution amplitudes $\phi(x,Q)$ which control large momentum transfer exclusive reactions (and directly coupled inclusive reactions) are each specific, basic measures of the ψ_n. Examples of these calculations are schematically illustrated in Figs. 1 through 3.

(4) Other physical quantities such as decay amplitudes provide rigorous sum rule or local constraints on the form of the valence components of meson and baryon wavefunctions.[2]

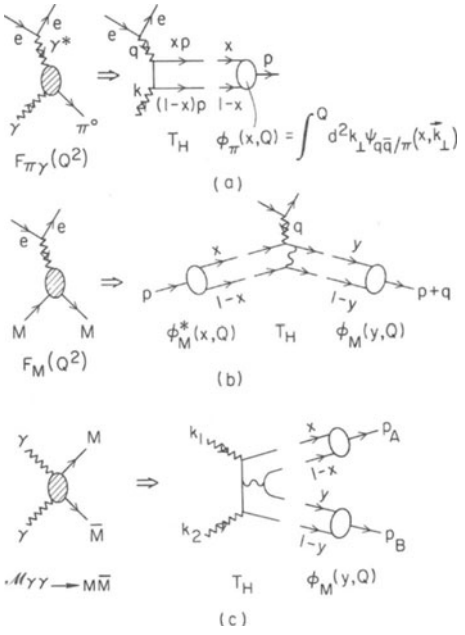

Fig. 1. Calculable large momentum transfer meson processes in QCD, and their connection to the meson Fock state wavefunction $\psi_{q\bar{q}}$ and distribution amplitude $\phi(x,Q)$. Only a representative diagram for the hard scattering amplitude T_H is shown. (a) The $\gamma \to \pi^o$ transition form factor (measurable in single tagged $ee \to ee\,\pi^o$ experiments), (b) the meson form factor, (c) the $\gamma\gamma \to M\bar{M}$ scattering amplitude. Details are discussed in Section IV.

The plan of these lectures is as follows. The basic derivations of (1) light-cone quantization, (2) the Fock state description of hadrons, (3) the meson form factors at large momentum transfer and distribution function evolution, (4) extensions to heavy atoms, and (5) the avoidance of scale and scheme ambiguities are presented in Lepage's lectures.[28] The main emphasis of the lectures in this chapter will be on novel methods and tools to probe hadronic structure, and the implications of phenomenological constraints on hadronic wavefunctions. In Sections II-IV we discuss measures of the hadronic wavefunction (form factors, magnetic moments, etc.),

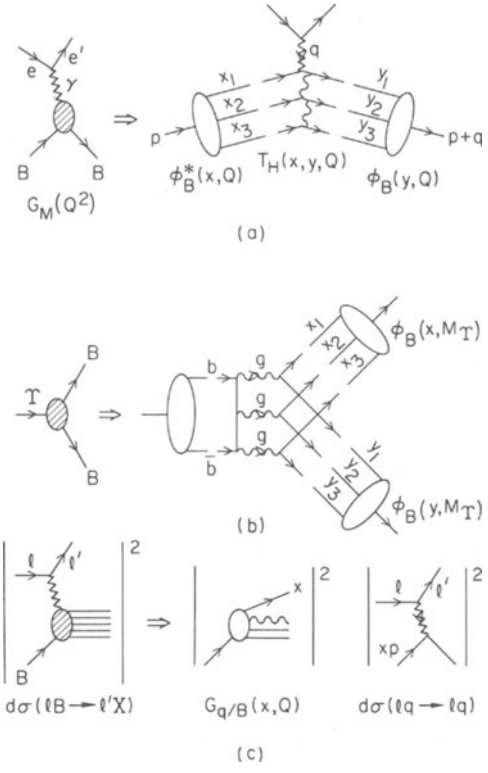

Fig. 2. Baryon processes at large momentum transfer in QCD and the connection to the baryon Fock state wavefunction. (a) Baryon form factors, (b) heavy quarkonium decay $T \to p\bar{p}$, (c) deep inelastic lepton-baryon scattering. Only representative contributions are shown. The inclusive cross section and structure function $G_{q/B}(x,Q)$ is computed from the square of the baryon wavefunction summed over all contributing Fock states.

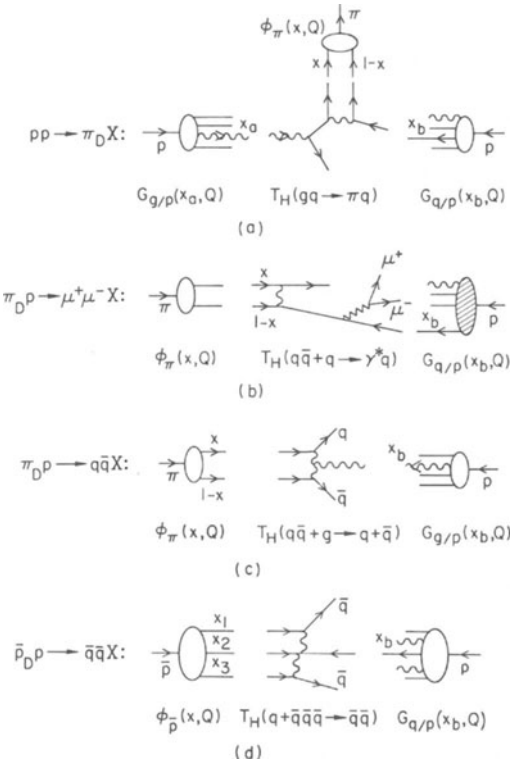

Fig. 3. Example of QCD-computable higher twist "direct-coupled" subprocesses for inclusive reactions. The subscript D indicates that the hadronic wavefunction is involved directly in the high momentum transfer subprocesses. (a) Direct production of high p_T mesons in hadron-hadron cross section. The predicted cross section is proportional to the meson form factor $F_M(p_T^2)$ times the leading twist cross section. (b) Higher twist contribution to meson-induced massive lepton pair production. The predicted cross section is equivalent to a contribution $F_L(x,Q^2) \sim C/Q^2$ to the longitudinal structure function of the meson. (c) Direct meson production of quark jets in meson-baryon collisions. All of the meson energy is used to produce jets at large transverse momentum. The cross section is proportional to $F_M(p_T^2)$ times the leading twist $qq \to qq$ cross section. (d) Direct production of anti-quark jets in $\bar{B}B$ collisions. The cross section is proportional to $G_M^B(p_T^2)$ times the leading twist $qq \to qq$ cross section. In each case the direct process dominates over the leading twist contribution in a large x kinematic region.

and give an abbreviated analysis of high momentum transfer exclusive processes. We also show how meson distribution amplitudes can be measured in $\gamma\gamma \to M\bar{M}$ reactions. The connection of the Fock state basis to leading and higher twist contributions to deep inelastic scattering is given in Section V. In Section VI we discuss how many different QCD processes are interrelated (as in Figs. 1 through 3) through the hadronic Fock states. We also discuss a novel type of QCD subprocesses — direct coupled hadron-induced reactions.[29] A new prediction for the proton form factor is also given. In Section VI, we also introduce a simple phenomenology of hadron wavefunctions and discuss present constraints on the form and normalization of the valence meson and nucleon Fock states. An important conclusion is that the valence Fock state as defined at equal time or the light cone appears to have a significantly smaller radius than that of the physical hadron;[27] higher Fock states thus play an essential role in low momentum transfer phenomenology. Applications to quark jet diffraction excitation[30] and the hidden heavy quark Fock state structure of hadrons are also discussed.[31-33]

II. HADRONIC WAVEFUNCTIONS IN QCD[27]

Even though quark and gluon perturbative subprocesses are simple in QCD, the complete description of a physical hadronic process requires the consideration of many different coherent and incoherent amplitudes, as well as the effects of non-perturbative phenomena[34] associated with the hadronic wavefunctions and color confinement. Despite this complexity, it is still possible to obtain predictions for many exclusive and inclusive reactions at large momentum transfer provided we make the ansatz that the effect of non-perturbative dynamics is negligible in the short-distance and far-off-shell domain. (This assumption appears reasonable since a linear confining potential $V \sim r$ is negligible compared to perturbative $1/r$ contributions.) For many large momentum transfer processes, such as deep inelastic lepton-hadron scattering reactions and meson form factors, one can then rigorously isolate the long-distance confinement dynamics from the short distance quark and gluon dynamics — at least to leading order in $1/Q^2$.[35] The essential QCD dynamics can thus be computed from (irreducible) quark and gluon subprocesses amplitudes as a perturbative expansion in an asymptotically small coupling constant $\alpha_s(Q^2)$.

An essential part of the QCD predictions is the hadronic wavefunctions which determine the probability amplitudes and distributions of the quark and gluons which enter the short distance subprocesses. The hadronic wavefunctions provide the link between the long distance non-perturbative and short distance perturbative physics. Eventually, one can hope to compute the wavefunctions from the theory, e.g., from lattice[36-38] or bag models,[39] or directly from the QCD equations of motions, as we shall outline below.

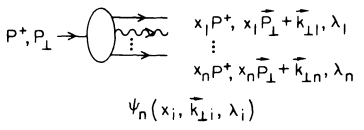

Fig. 4. The n-particle Fock state amplitude defined at equal τ.

Knowledge of hadronic wavefunction will also provide explicit connections between exclusive and inclusive processes,[40] and will allow the normalization and specification of the power law (higher twist) corrections to the leading impulse approximation results. As we shall discuss in Section VI, there are a number of novel QCD phenomena associated with hadronic wavefunctions, including the effects of intrinsic gluons, intrinsic heavy quark Fock components,[41] diffraction dissociation phenomena, and "direct" hadron processes where the valence Fock state of a hadron enters coherently into a short-distance quark-gluon subprocess.

The most convenient representation of a wavefunction in a relativistic field theory is to use a momentum space Fock state basis defined at equal "time" $\tau = t + z$ on the light cone (see Fig. 4):[42]

$$\{\psi_n(\vec{k}_{\perp i}, x_i; \lambda_i)\}. \tag{2.1}$$

Momentum conservation requires

$$\sum_{i=1}^{n} \vec{k}_{\perp i} = 0 , \qquad \sum_{i=1}^{n} x_i = 1 , \qquad 0 < x_i < 1 . \tag{2.2}$$

The $\vec{k}_{\perp i}$ are the transverse momentum of the (on-mass-shell) constituents relative to the bound state 3-momentum $\vec{P} = P^3\hat{z}$. The x_i are the light-cone momentum fractions ($k^\pm = k^o \pm k^3$, $A\cdot B = \frac{1}{2}(A^+B^- + A^-B^+) - \vec{A}_\perp \cdot \vec{B}_\perp$

$$x_i = \frac{k_i^+}{P^+} = \frac{(k^o + k^3)_i}{P^o + P^3} \quad . \tag{2.3}$$

(In a frame where $P^3 \to \infty$, the x_i are the longitudinal momentum fractions.) The mass shell condition is $k^2 = m^2$, or $k^- = (k_\perp^2 + m^2)/k^+$. As we shall see, the equal-τ formalism is equivalent to the usual Schroedinger equal-time theory in the non-relativistic limit.

A unique and remarkable advantage of quantizing a relativistic theory at equal τ is the fact that the perturbative vacuum state $|0\rangle$ is also an eigenstate of the full Hamiltonian. Matrix elements where particles are created out of the vacuum are excluded because of the fact that all particles must have $k_i^+ > 0$. Furthermore,

the charge operator and the current $J^+ = J^o + J^3$ are diagonal in the Fock state basis. It is particularly advantageous to choose the light-cone gauge $A^+ = A^o + A^3 = 0$ since unphysical degrees of freedom do not appear. A comparison between time-ordered and τ-ordered perturbation theory is given in Table I.

Calculations in light-cone perturbation theory are often surprisingly simple since one can usually choose Lorentz frames for the external particles such that only a few time-orderings need to be considered.[43-44] All the variables have a direct physical interpretation. The formalism is also ideal for computing helicity amplitudes directly without trace projection techniques. A list of all the gluon fermion vertices which are required as gauge theory calculations is given in Tables I and II of Reference 19. Further details and derivations may be found in Lepage's lectures in this volume.

Table I. Time-ordered perturbation theory.

Equal t	Equal $\tau = t + z$
$k^o = \sqrt{\vec{k}^2 + m^2}$ $\begin{pmatrix}\text{particle}\\ \text{mass shell}\end{pmatrix}$	$k^- = \frac{k^2 + m^2}{k^+}$ $\begin{pmatrix}\text{particle}\\ \text{mass shell}\end{pmatrix}$
$\sum \vec{k}$ conserved	$\sum \vec{k}_\perp, k^+$ conserved
$\mathcal{M}_{ab} = V_{ab} + \sum_c V_{ac} \frac{1}{\sum_a k^o - \sum_c k^o + i\varepsilon} V_{cb}$	$\mathcal{M}_{ab} = V_{ab} + \sum_c V_{ac} \frac{1}{\sum_a k^- - \sum_c k^- + i\varepsilon} V_{cb}$
n! time-ordered contributions	$k^+ > 0$ only
Fock states $\psi_n(\vec{k}_i)$	Fock states $\psi_n(\vec{k}_{\perp i}, x_i)$
$\sum_{i=1}^n \vec{k}_i = \vec{P} = 0$	$x = \frac{k^+}{P^+}$, $\sum_{i=1}^n x_i = 1$, $\sum_{i=1}^n \vec{k}_{\perp i} = 0$
	$(0 < x_i < 1)$
$\mathcal{E} = P^o - \sum_{i=1}^n k_i^o$	$\mathcal{E} = P^+(P^- - \sum_{i=1}^n k_i^-)$
$= M - \sum_{i=1}^n \sqrt{k_i^2 + m_i^2}$	$= M^2 - \sum_{i=1}^n \left(\frac{k_\perp^2 + m^2}{x}\right)_i$

It is straightforward to implement ultraviolet renormalization in light-cone perturbation theory. We define truncated wavefunctions ψ^κ and a truncated Hamiltonian H^κ such that all intermediate states with $|\mathcal{E}| > \kappa^2$ are excluded.[45] Thus κ^{-1} is analogous to the lattice spacing in lattice field theory. Since QCD is renormalizable the effects of the neglected states are accounted for by the use of the running coupling constant $\alpha_s(\kappa^2)$ and running mass $m(\kappa^2)$, as long as κ^2 is sufficiently large compared to all physical mass thresholds. Completeness implies

$$\sum_{n,\lambda_i} \int [d^2k_\perp] \int [dx] |\psi_n^\kappa(x_i, k_{\perp i}; \lambda_i)|^2 = 1 - O\left(\frac{m^2}{\kappa^2}\right) \tag{2.4}$$

$$[d^2k_\perp] = 16\pi^3 \delta^2\left(\sum_{i=1}^{n} \vec{k}_{\perp i}\right) \prod_{i=1}^{n} \frac{d^2k_{\perp i}}{16\pi^3} \tag{2.5}$$

and

$$[dx] = \delta\left(1 - \sum_{i=1}^{n} x_i\right) \prod_{i=1}^{n} dx_i \quad . \tag{2.6}$$

The equation of motion for the meson or baryon wavefunction in QCD is a set of coupled multiparticle equations (see Fig. 5):

$$\left(M^2 - \sum_{i=1}^{n} \left(\frac{k_\perp^2 + m^2}{x}\right)_i\right) \psi_n^\kappa = \sum_{n'} V_{nn'}^\kappa \psi_{n'}^\kappa \quad , \tag{2.7}$$

where M^2 is the eigenvalue and $V_{nn'}$ is the set of diagonal (from instantaneous gluon and fermion exchange) and off-diagonal (from the 3 and 4 particle vertices) momentum-space matrix elements dictated by the QCD rules. Because of the κ cutoff the equations truncate at finite n,n'. In analogy to non-relativistic theory, one can imagine starting with a trial wavefunction for the lowest $|q\bar{q}\rangle$ or $|qqq\rangle$ valence state of a meson or baryon and iterating the equations of motion to determine the lowest eigenstate Fock state wavefunctions and mass M. Invariance under changes in the cutoff scale provides an important check on the consistency of the results. Note that the general solution for the hadron wavefunction in QCD

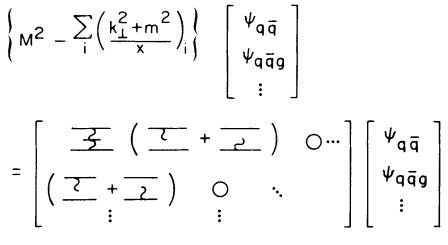

Fig. 5. QCD equation of motion for meson wavefunction.

is expected to have Fock state components with arbitrary numbers of gluons and quark-antiquark pairs.

We can make an (approximate) connection between the equal-time wavefunction of a composite system and the light-cone wavefunction by equating the off-shell propagator $\mathcal{E} = M^2 - (\sum_{i=1}^{n} k_i)^2$ in the two frames:

$$\mathcal{E} = \begin{cases} M^2 - \left(\sum_{i=1}^{n} q^o_{(i)}\right)^2 , & \sum_{i=1}^{n} q_i = 0 \text{[C.M.]} \\ M^2 - \sum_{i=1}^{n} \left(\frac{k_\perp^2 + m^2}{x}\right)_i , & \sum \vec{k}_{\perp i} = 0 , \ \sum x_i = 1 \text{[L.C.]} \end{cases} . \tag{2.8}$$

In addition we can identify

$$x_i = \frac{k_i^+}{p^+} \rightleftarrows \frac{q^o + q^3_i}{\sum_{j=1}^{n} q^o_{(j)}} , \qquad \vec{k}_{\perp i} \rightleftarrows \vec{q}_{\perp i} . \tag{2.9}$$

For a relativistic two particle state with a wavefunction which is a function of the off-shell variable $\mathcal{E}$ only, then we can identify $(m_1 = m_2 = m, \ x = x_1 - x_2)$[27]

$$\psi_{\text{L.C.}}\left(\frac{k_\perp^2 + m^2}{1 - x^2} - m^2\right) \rightleftarrows \psi_{\text{C.M.}}(\vec{q}^2) . \tag{2.10}$$

In the non-relativistic limit this corresponds to the identification $\vec{q}_\perp = \vec{k}_\perp$, $q_3^2 = x^2 m^2$.

III. MEASURES OF HADRONIC WAVE FUNCTIONS

A. Form Factors of Composite Systems

If we could solve the QCD equation of state [Eq. (2.7)] for the light-cone wavefunctions ψ_n of a hadron then we could (in principle) calculate all of its electromagnetic properties. For example, to compute the elastic form factors $\langle p|J^\mu(0)|p+q\rangle$ of a hadron we choose the Lorentz frame[46]

$$\begin{aligned} p^\mu &= (p^+, p^-, \vec{p}_\perp) = (p^+, \frac{M^2}{p^+}, \vec{0}_\perp) \\ q^\mu &= (q^+, q^-, \vec{q}_\perp) = (0, \frac{2p\cdot q}{p^+}, \vec{q}_\perp) \end{aligned} \tag{3.1}$$

where $p^2 = (p+q)^2 = M^2$ and $-q^2 = Q^2 = \vec{q}_\perp^{\,2}$. Then the only time ordering

which contributes to the $\langle p|J^+|p+q\rangle$ matrix element is where the photon attaches directly to the $e_j\bar{u}_j\gamma^+u_j$ currents of the constituent quarks. The spin averaged form factor is[46,19] (see Fig. 6a)

$$F(Q^2) = \sum_n \sum_j e_j \int [dx][d^2k_\perp] \sum_{\lambda_i} \psi_n^{*\kappa}(x_i, \vec{k}'_{\perp i}; \lambda_i)\psi_n^{\kappa}(x_i, \vec{k}_{\perp i}; \lambda_i) \quad (3.2)$$

where $\vec{k}_j^{\perp\prime} = \vec{k}_j^{\perp} + (1-x_j)\vec{q}^{\perp}$ for the struck quark and $\vec{k}_i^{\perp} - x_i\vec{q}^{\perp}$ $(i \neq j)$ for the spectator quarks. (The $-x_i\vec{q}^{\perp}$ terms occur because the arguments $\vec{k}^{\perp\prime}$ are calculated relative to the direction of the final state hadron.) We choose $\kappa^2 >> Q^2, M^2$. We note here the special advantage of light-cone perturbation theory: the current J^+ is diagonal in the Fock state basis.

Because of Eq. (2.4) the form factor is normalized to 1 at zero momentum transfer. We can also compute the helicity flip form factors in the same manner.[19,47] For example, the anomalous moment $a = F_2(0)$ of any spin 1/2 system can be written[47]

$$\frac{a}{M} = -\sum_j e_j \int [dx][d^2k_\perp]\psi^{*\kappa}_{p\uparrow} \sum_{i\neq j} x_j \left(\frac{\partial}{\partial k_i^1} + i\frac{\partial}{\partial k_i^2}\right)\psi^{\kappa}_{p\downarrow} \quad . \quad (3.3)$$

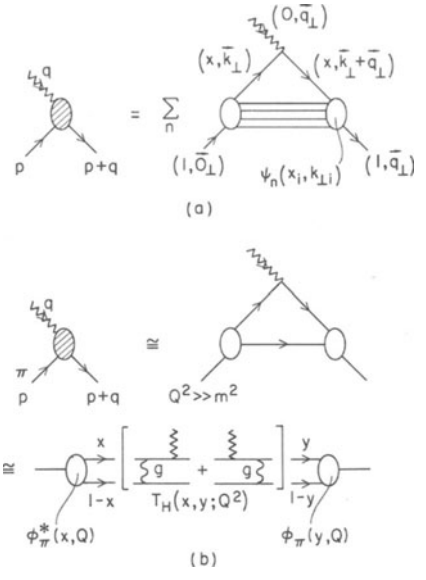

Fig. 6. (a) Calculation of current matrix elements in light-cone perturbation theory. (b) Valence Fock state contribution to the large momentum transfer meson form factor. T_H is computed for zero mass quarks q and $\bar{q}$ parallel to the pion momentum.

Explicit calculations of the electron anomalous moment in QED using this result are given in Reference 47. We notice that in general all Fock states ψ_n^κ contribute to the anomalous moment of a system, although states with κ^2 much larger than the mean off shell energy $<\mathcal{E}>$ are not expected to be important. The general result (3.3) also includes the effects of the Lorentz boost of the wavefunction from p^μ to $(p+q)^\mu$. In particular, the Wigner spin rotation contributes to $F_2(q^2)$ and the charge radius $F_1'(q^2)$ in the $q^2 \to 0$ limit and can only be neglected in the limit of non-relativistic binding $<\varepsilon> << M^2$. This effect gives non-trivial relativistic corrections[48] to nuclear magnetic moment calculations based on simple additivity $\vec{\mu} = <\sum_j \vec{\mu}_j>$.

B. Form Factors of Mesons*

Results such as Eqs. (3.2) and (3.3) are formally exact but useless unless we have complete knowledge of the hadronic or nuclear wavefunction. However, by making use of the impulse approximation and the smallness of the QCD running coupling constant, we can calculate features of elastic and inelastic large momentum transfer processes[19] without explicit knowledge of the wavefunction. For example, consider the $|q\bar{q}>$ Fock state component contribution to the pion form factor. Choosing $\kappa^2 = Q^2$, we have

$$F_\pi(Q^2) = \int_0^1 dx \int^Q \frac{d^2k_\perp}{16\pi^3} \psi^{*Q}(x,\vec{k}_\perp)\psi^Q(x,\vec{k}_\perp + (1-x)\vec{q}_\perp)$$

$$+ \text{higher Fock state contributions} . \qquad (3.4)$$

The bound state wavefunctions are peaked at low transverse momentum, i.e., small off-shell energy $\mathcal{E}$. Thus the leading contribution at large Q^2 come from the regimes (a) $\vec{k}_\perp^2 << \vec{q}_\perp^2$ and (b) $(\vec{k}_\perp + (1-x)\vec{q}_\perp)^2 << \vec{q}_\perp^2$. Thus

$$F_\pi^{(a)}(Q) \simeq \int_0^1 dx\ \phi(x,Q)\ \psi^Q(x,(1-x)\vec{q}_\perp) \qquad (3.5)$$

where[19]

$$\phi(x,Q) \equiv \int^Q \frac{d^2k_\perp}{16\pi^3} \psi^Q(x,k_\perp) \quad . \qquad (3.6)$$

If we simply iterate the one-gluon exchange kernel V_1 in the equation of motion for ψ, then for $q_\perp^2 << <\ell_\perp^2>$

*Further discussion may be found in Lepage's lectures in this volume and Refs. 11 and 19.

$$\psi^Q(x,(1-x)q_\perp) \cong \int_0^1 dy \int^Q \frac{d^2\ell_\perp}{16\pi^3} \frac{V_1(x,(1-x)q_\perp;y,\ell_\perp)\psi^Q(y,\ell_\perp)}{-q_\perp^2(1-x)/x}$$

$$\cong \int_0^1 dy \frac{V_1(x,(1-x)q_\perp;y,0_\perp)}{-q_\perp^2(1-x)/x} \phi(y,Q) \quad . \tag{3.7}$$

Thus we can write the gluon exchange contribution to the form factor in the form;[11,19] [see Fig. 6b)]

$$F_\pi(Q^2) = \int_0^1 dx\, dy\, \phi^*(y,Q)\, T_H(x,y;Q)\, \phi(y,Q) \tag{3.8}$$

where

$$T_H = \frac{16\pi C_F \alpha_s(Q^2)}{Q^2} \left(\frac{e_1}{(1-y)(1-x)} + \frac{e_2}{xy}\right) \tag{3.9}$$

is the "hard scattering amplitude" for scattering collinear constituents q and $\bar{q}$ from the initial to the final direction. The color factor is $C_F = \frac{1}{2n_c}(n_c^2 - 1) = 4/3$. The "distribution amplitude" $\phi(x,Q)$ is the amplitude for finding the $|q\bar{q}>$ Fock state in the pion collinear up to the scale Q. (It is analogous to the wavefunction at the origin in non-relativistic calculations.) The distribution amplitude enters universally in all large momentum transfer exclusive amplitude and is a process-independent measure of the valence quark distribution in each hadron; its (logarithmic) dependence on Q^2 can be determined directly from the operator product expansion or the light-cone or from an evolution equation, as we discuss below.

Thus the simplest estimate for the asymptotic behavior of the meson form factor is $F_\pi(Q^2) \sim \alpha_s(Q^2)/Q^2$. To see if this is correct we must examine the higher order corrections:[19]

(1) Contributions from higher particle number Fock states $|q\bar{q}g>$, $|q\bar{q}q\bar{q}>$, etc. are power-law suppressed since (in light-cone gauge) the numerator couplings cannot compensate the extra fall-off in Q^2 from the extra energy denominators.

(2) All infrared singularities and contributions from soft ($\ell_\perp \to 0$) gluons cancel in color singlet matrix elements. [It is interesting to note that the quark (Sudakov) form factor falls faster at large Q^2 than $F_\pi(Q^2)$.]

(3) Vertex and vacuum polarization corrections to T_H are higher order in $\alpha_s(Q^2)$ since we choose $\kappa^2 = Q^2$. The effective argument of α_s

in T_H is $Q^2 = xy\,Q^2$ or $(1-x)(1-y)Q^2$ corresponding to the actual momentum transfer carried by the gluon.

(4) By definition, $\phi(x,\kappa^2)$ sums all (reducible) contributions from low momentum transfer gluon exchange in the $q\bar{q}$ wavefunction. Hard gluon contributions with $|\mathcal{E}| > \kappa^2$ and the irreducible (cross-graph, etc.) give contributions to T_H which are higher order $\alpha_s(Q^2)$. By analyzing the denominators in T_H one can show that the natural $\mathcal{E}$ cutoff for $\phi(x,\kappa)$ which minimizes higher order contributions is $\kappa^2 = Q_x^2 = Q^2 \min\{\frac{x}{1-x}, \frac{1-x}{x}\}$.

(5) Although T_H is singular at $x \to 0,1$, the endpoint behavior of $\phi(x,Q^2) \sim x^\varepsilon$, $(1-x)^\varepsilon$ $(\varepsilon > 0)$ is sufficient to render this region harmless.

C. The Meson Distribution Amplitude

The essential prediction of QCD for the pion form factor is the power-law behavior[8] $F_\pi \sim 1/Q^2$, with logarithmic corrections from the explicit powers of $\alpha_s(Q^2)$ in T_H and the Q^2 dependence of the distribution amplitude $\phi(x,Q^2)$.

The variation of ϕ with Q^2 comes from the upper limit of the $\vec{k}_\perp$ integration (since $\psi \sim 1/k_\perp^2$) and the renormalization scale dependence:

$$\psi^Q(x,\vec{k}_\perp) = \frac{Z_2(Q)}{Z_2(Q_o)}\,\psi^{Q_o}(x,\vec{k}_\perp) \tag{3.10}$$

due to vertex and self-energy insertions. Thus

$$Q^2\frac{\partial}{\partial Q^2}\phi(x,Q) = \frac{Q^2}{16\pi^2}\psi^Q(x,\vec{q}_\perp) + \frac{d}{d\log Q^2}\log Z_2(Q^2)\phi(x,Q)\,. \tag{3.11}$$

To order $\alpha_s(Q^2)$ we can compute $Q^2\psi$ from one-gluon exchange [as in Eq. (3.7)], and $d\log Z_2(Q^2)/d\log Q^2 = \alpha_s(Q^2)\gamma_F/4\pi$. Setting $\phi(x,Q) = x(1-x)\tilde{\phi}(x,Q) = x_1x_2\tilde{\phi}$, we obtain an "evolution equation"

$$x_1x_2Q^2\frac{\partial}{\partial \log Q^2}\tilde{\phi}(x_i,Q) = \frac{\alpha_s(Q^2)}{4\pi}\int_0^1 [dy]\,V(x_i,y_i)\phi(y,Q) \tag{3.12}$$

where

$$V(x_i,y_i) = 2C_F\left\{x_1y_2\theta(y_1-x_1)\left(\delta_{h_1\bar{h}_2} + \frac{\Delta}{y_1-x_1}\right) + (1 \leftrightarrow 2)\right\} \tag{3.13}$$

$[\delta_{h_1\bar{h}_2} = 1$ when the q and $\bar{q}$ helicities are opposite] and

$$\Delta\tilde{\phi}(y_i,\zeta) = \tilde{\phi}(y_i,Q) - \tilde{\phi}(x_i,Q)\,. \tag{3.14}$$

The $\tilde{\phi}(x_1,Q)$ subtraction is due to the $\gamma_F\phi$ term — i.e., the infrared dependence at $y_i = x_i$ is cancelled for color singlet hadrons. Thus given the initial condition $\phi(x_i,Q_o)$, perturbation theory determines the evolution of $\phi(x,Q)$ for $Q > Q_o$. The solution to the evolution equation is[19]

$$\phi(x_i,Q) = x_1 x_2 \sum_{n=0}^{\infty} a_n(Q_o^2)\, C_n^{3/2}(x_1-x_2)(\log Q^2/\Lambda^2)^{-\gamma_n} \qquad (3.15)$$

where the Gegenbauer polynomials $C_n^{3/2}$ (orthogonal on $\int [dx] x_1 x_2$) are eigenfunctions of $V(x_i,y_i)$. The corresponding eigenvalues are the "non-singlet" anomalous dimensions:

$$\gamma_n = \frac{C_F}{\beta_o}\left[1 + 4\sum_{2}^{n+1}\frac{1}{k} - \frac{2\delta_{h_1\bar{h}_2}}{(n+1)(n+2)}\right] \geq 0 \quad . \qquad (3.16)$$

[These results can also be derived by using the operator product expansion for the distribution amplitude.[49] By definition

$$\phi(x,Q) = \Lambda^+ \int \frac{dz^-}{2\pi}\, e^{ixz^-/2}\, i\langle 0|\bar{\psi}(z)\psi(0)|\pi\rangle^Q\Big|_{z^+=0,\, z^2=-z_\perp^2=O(-1/Q^2)} \qquad (3.17)$$

(Λ^+ is the positive energy spinor projection operator). The relative separation of the q and $\bar{q}$ thus approaches the light-cone $z^2 = 0$ as $Q^2 \to \infty$. Equation (3.16) then follows, by expanding $\psi(z)\psi(0)$ in local operators.]

The coefficients a_n are determined from $\phi(x_i,Q_o)$:

$$a_n\left[\log\frac{Q^2}{\Lambda^2}\right]^{-\gamma_n} = \frac{2(2n+3)}{(2+n)(1+n)}\int_{-1}^{1} d(x_1-x_2)\, C_n^{3/2}(x_1-x_2)\phi(x_i,Q_o). \qquad (3.18)$$

For $Q^2 \to \infty$, only the leading $\gamma_o = 0$ term survives:

$$\lim_{Q^2\to\infty}\phi(x,Q) = a_o x_1 x_2 \qquad (3.19)$$

where

$$\frac{a_o}{6} = \int_0^1 dx\, \phi(x,Q) = \int_0^1 dx \int^Q \frac{d^2k_\perp}{16\pi^3}\,\psi^Q(x,k_\perp) \qquad (3.20)$$

is the meson wavefunction at the origin as measured in the decay $\pi \to \mu\nu$:

$$\frac{a_o}{6} = \frac{1}{2\sqrt{n_c}}\, f_\pi \quad . \qquad (3.21)$$

More generally, the leptonic decay ($\rho^o \to e^+e^-$, etc.) of each meson normalizes its distribution amplitude by the "sum rule"

$$\int_0^1 dx\ \phi_M(x,Q) = \frac{f_M}{2\sqrt{n_c}} \quad , \tag{3.22}$$

independent of Q. The fact that $f_\pi \neq 0$ implies that the probability of finding the $|q\bar{q}>$ Fock state in the pion is non-zero. In fact all the Fock states wavefunctions $\psi_n^K(x_i,k_{\perp i})$ ($|\mathcal{E}| < \kappa^2$) are well-defined, even in the infrared limit $x_i \to 0$ (since $|\mathcal{E}| \sim <k_\perp^2>/x_i$ and $<k_\perp^2>$ is non-zero for a state of finite radius).

The pion form factor at high Q^2 can thus be written[11,19,50]

$$F_\pi(Q^2) = \int_0^1 dx\ \phi^*(x,Q)\ T_H(x,y;Q)\ \phi(y,Q)$$
$$T_H = \frac{16}{3\pi}\ \frac{\alpha_s((1-x)(1-y)Q^2)}{(1-x)(1-y)Q^2} \quad . \tag{3.23}$$

Thus

$$F_\pi(Q^2) = \left| \sum_{n=0} a_n (\log Q^2/\Lambda^2)^{-\gamma_n} \right|^2 \frac{16\pi}{3}\ \frac{\alpha_s(\bar{Q}^2)}{Q^2}$$
$$\times \left(1 + O(\frac{\alpha_s(Q^2)}{\pi}) + O(\frac{m^2}{Q^2})\right) \tag{3.24}$$

where $\bar{Q}^2 \cong <(1-x)(1-y)>Q^2$. Finally, for the asymptotic limit where only the leading anomalous dimension contributes:[51]

$$\lim_{Q^2\to\infty} F_\pi(Q^2) = 16\pi\, f_\pi^2\ \frac{\alpha_s(Q^2)}{Q^2} \quad . \tag{3.25}$$

The analysis of the $F_{\pi\gamma}(Q^2)$ form factor, measurable in $ee \to ee\pi^o$ reactions proceeds in a similar manner. [See Fig. 1(a).] An interesting result is[19]

$$\alpha_s(Q^2) = \frac{F_\pi(Q^2)}{4\pi Q^2 |F_{\pi\gamma}(Q^2)|^2} \left(1 + O(\frac{\alpha_s(Q^2)}{\pi})\right) \tag{3.26}$$

which provides a definition of α_s independent of the form of the distribution function ϕ_π. Higher order corrections to $F_\pi(Q^2)$ and $F_{\pi\gamma}(Q^2)$ are discussed in Reference 50.

IV. LARGE MOMENTUM TRANSFER EXCLUSIVE PROCESSES[19]

The meson form factor calculation which we outlined above is the prototype for the calculation of the QCD hard scattering contribution for the whole range of exclusive processes at large momentum transfer. Away from possible special points in the x_i

integrations (see below) a general hadronic amplitude can be written to leading order in $1/Q^2$ as a convolution of a connected hard-scattering amplitude T_H convoluted with the meson and baryon distribution amplitudes:

$$\phi_M(x,Q) = \int^{|\mathcal{E}|<Q^2} \frac{d^2k_\perp}{16\pi^2} \psi^Q_{q\bar{q}}(x,\vec{k}_\perp) \quad , \tag{4.1}$$

and

$$\phi_B(x_i,Q) = \int^{|\mathcal{E}|<Q^2} [d^2k_\perp]\psi_{qqq}(x_i,\vec{k}_{\perp i}) \quad . \tag{4.2}$$

The hard scattering amplitude T_H is computed by replacing each external hadron line by massless valence quarks each collinear with the hadrons momentum $P_i^\mu \cong x_i P_H^\mu$. For example the baryon form factor at large Q^2 has the form[9,19] [see Figs. 2(a) and 7]

$$G_M(Q^2) = \int [dx]\ [dy]\ \phi^*(y_i,\bar{Q})\ T_H(x,y;Q^2)\ \phi(x,\bar{Q}) \tag{4.3}$$

where T_H is the $3q + \gamma \to 3q'$ amplitude. [The optimal choice for $\bar{Q}$ is discussed in Reference 19.] For the proton and neutron we have to leading order [$C_B = 2/3$]

$$T_p = \frac{128\pi^2\, C_B^2}{(Q^2+M_o^2)^2}\ T_1 \tag{4.4}$$

$$T_n = \frac{128\pi^2\, C_B^2}{3(Q^2+M_o^2)^2}\ [T_1 - T_2] \tag{4.5}$$

where

$$T_1 = -\frac{\alpha_s(x_3y_3Q^2)\alpha_s((1-x_1)(1-y_1)Q^2)}{x_3(1-x_1)^2\ y_3(1-y_1)^2} + \frac{\alpha_s(x_2y_2Q^2)\alpha_s((1-x_1)(1-y_1)Q^2)}{x_2(1-x_1)^2\ y_2(1-y_1)^2}$$

$$- \frac{\alpha_s(x_2y_2Q^2)\alpha_s(x_3y_3Q^2)}{x_2x_3(1-x_3)y_2y_3(1-y_1)} \quad , \tag{4.6}$$

and

$$T_2 = -\frac{\alpha_s(x_1y_1Q^2)\alpha_s(x_3y_3Q^2)}{x_1x_3(1-x_1)y_1y_3(1-y_3)} \quad . \tag{4.7}$$

T_1 corresponds to the amplitude where the photon interacts with the quarks (1) and (2) which have helicity parallel to the nucleon helicity, and T_2 corresponds to the amplitude where the quark with opposite helicity is struck. The running coupling constants have arguments $\hat{Q}^2$ corresponding to the gluon momentum transfer of each diagram. Only the large Q^2 behavior is predicted by the theory;

we utilize the parameter M_o to represent the effect of power-law suppressed terms from mass insertions, higher Fock states, etc.

The Q^2-evolution of the baryon distribution amplitude can be derived from the operator product expansion of three quark fields or from the gluon exchange kernel, in parallel with the derivation of (3.12). The baryon evolution equation to leading order in α_s is[19]

$$x_1x_2x_3\left\{\frac{\partial}{\partial\zeta}\tilde{\phi}(x_i,Q)+\frac{3}{2}\frac{C_F}{\beta_o}\tilde{\phi}(x_i,Q)\right\}=\frac{C_B}{\beta_o}\int_0^1[dy]V(x_i,y_i)\tilde{\phi}(y_i,Q). \quad (4.8)$$

Here $\phi=x_1x_2x_3\tilde{\phi}$, $\zeta=\log(\log(Q^2/\Lambda^2)$ and [see Fig. 7(b)]

$$V(x_i,y_i) = 2x_1x_2x_3\sum_{i\neq j}\theta(y_i-x_i)\delta(x_k-y_k)\frac{y_j}{x_j}\left(\frac{\delta h_i\bar{h}_j}{x_i+x_j}+\frac{\Delta}{y_i-x_i}\right)$$
$$= V(y_i,x_i)\ . \quad (4.9)$$

The infrared singularity at $x_i=y_i$ is cancelled because the baryon is color singlet. The evolution equation has the general solution

$$\phi(x_i,Q) = x_1x_2x_3\sum_{n=0}^{\infty}a_n\,\tilde{\phi}_n(x_i)\left(\log\frac{Q^2}{\Lambda^2}\right)^{-\gamma_n^B}\ . \quad (4.10)$$

The leading (polynomial) eigensolution $\tilde{\phi}_n(x_i)$ and corresponding baryon anomalous dimensions are given in References 19 and 52. Thus at large Q^2, the nucleon magnetic form factors have the form[9,19]

$$G_M(Q^2)\to\frac{\alpha_s(Q^2)}{Q^4}\sum_{n,m}b_{nm}\left(\log\frac{Q^2}{\Lambda^2}\right)^{-\gamma_n^B-\gamma_m^B}\left(1+O(\alpha_s(Q^2),\frac{m^2}{Q^2})\right). \quad (4.11)$$

We can also use this result to obtain results for ratios of various baryon and isobar form factors assuming isospins or SU(3)-flavor

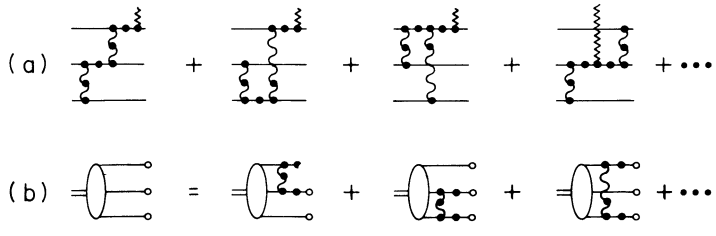

Fig. 7. (a) Leading contributions to T_H for the baryon form factors corresponding to the four terms of Eqs. (4.6) and (4.7), respectively. (b) Contributions to the kernel for the evolution of the baryon distribution amplitude.

symmetry for the basic wavefunction structure. Results for the neutral weak and charged weak form factors assuming standard SU(2) ×U(1) symmetry are given in Reference 46.

As we see from Eq. (4.3), the integration over x_i and y_i have potential endpoint singularities. However, it is easily seen that any anomalous contribution [e.g., from the region $x_2, x_3 \sim O(m/Q)$, $x_1 \sim 1 - O(m/Q)$] is asymptotically suppressed at large Q^2 by a Sudakov form factor arising from the virtual correction to the $\bar{q}\gamma q$ vertex when the quark legs are near-on-shell [$p^2 \sim O(mQ)$].[19,53] This Sudakov suppression of the endpoint region requires an all orders resummation of perturbative contributions,[54] and thus the derivation of the baryon form factors is not as rigorous as for the meson form factor, which has no such endpoint singularity.

The most striking feature of the QCD prediction (4.11) is the $1/Q^4$ power-law behavior of G_M^p as G_M^n. The power-law dependence reflects:

(1) The essential scale-invariance of the qq scattering subprocesses within T_H.

(2) The fact that the minimal Fock state of a baryon is the 3-quark state.

We will discuss the phenomenology of the baryon form factors and the resulting constraints on the baryon wavefunction in Section VI.

In the case of hadron scattering amplitudes A+B → C+D, photoproduction, Compton scattering, etc., the leading hard scattering QCD contribution at large momentum transfer $Q^2 = tu/s$ has the form[19] (helicity labels and suppressed) (see Fig. 8)

$$\mathcal{M}_{A+B \to C+D}(Q^2, \theta_{c.m.}) = \int [dx] \phi_C(x_c, \tilde{Q}) \phi_D(x_d, \tilde{Q}) T_H(x_i; Q^2, \theta_{c.m.}) \times \phi_A(x_a, \tilde{Q}) \phi_B(x_b, \tilde{Q}) \quad . \tag{4.12}$$

The essential behavior of the amplitude is determined by T_H, computed where each hadron is replaced by its (collinear) quark constituents. We note again that T_H is "collinear irreducible," i.e., the transverse momentum integrations of all reducible loop integration are restricted to $k_\perp^2 > O(Q^2)$ since the small $k_\perp$ region is already contained in ϕ. If the internal propagators in T_H are all far-off-shell $O(Q^2)$ [as in Fig. 8(a)] then a perturbative expansion in $\alpha_s(Q^2)$ can be carried out. However, this is not true for all hadron-hadron scattering amplitudes since one can have multiple quark-quark scattering processes which allow near-on-shell propagation in intermediate states at finite values of the x_i.[17]

The classic example is meson-meson scattering, where two pairs of quarks scatter through the same angle [see Fig. 8(c)]. However, the near-on-shell region of integration is again suppressed by Sudakov factors. [Physically this suppression occurs because the near-on-shell quarks must scatter without radiating gluons.] A model calculation by Mueller[10] for π-π scattering in QCD (using an exponentiated form of the Sudakov form factor) shows that the leading contribution comes in fact from the off-shell region $|k^2| \sim O(Q^2)^{1-\epsilon}$ where $\epsilon = (2c+1)^{-1}$, $c = 8C_F/(11 - \frac{2}{3} n_f)$ (for four flavors $\epsilon \cong 0.281$). This region gives the contribution

$$\mathcal{M}_{\pi\pi \to \pi\pi} \sim O(Q^2)^{-3/2 - c \ln(2c+1/2c)} \cong (Q^2)^{-1.922} \tag{4.13}$$

compared to $(Q^2)^{-2}$ from the hard scattering $|k^2| \sim O(Q^2)$ region.

Thus even when pinch singularities are present the far-off-shell hard scattering quark and gluon processes dominate large momentum transfer hadron scattering amplitudes: Given this result we can abstract some general QCD features common to all exclusive processes at large momentum transfer:

(1) All of the non-perturbative bound state physics is isolated in the process-independent distribution amplitudes.

(2) The nominal power-law behavior of an exchange amplitude is $(1/Q)^{n-4}$ where n is the number of external elementary particles (quarks, gluons, leptons, photons in T_H). This immediately implies the dimensional counting rules:

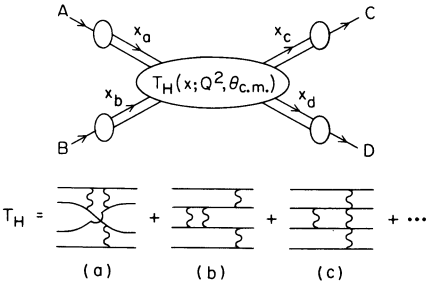

Fig. 8. QCD contributions to meson-meson scattering at large momentum transfer. Diagram (c) corresponds to the Landshoff pinch singularity which is suppressed by quark form factor effects.

$$\frac{d\sigma}{dt}\,(A+B \to C+D) \sim \left(\frac{1}{Q^2}\right)^{n-2} f(\theta_{c.m.}) \tag{4.14}$$

where $n = n_A + n_B + n_C + n_D$, and

$$F_H(Q^2) \sim \left(\frac{1}{Q^2}\right)^{n_H - 1} \tag{4.15}$$

where F_H is the helicity-conserving[18,19] form factor. These power-law predictions are modified by (a) the Q^2-dependence of the factors of α_s in T_H, (b) the Q^2-evolution of the distribution amplitudes and (c) a possible small power associated with the almost complete Sudakov suppression of pinch singularities in hadron-hadron scattering. The dimensional-counting rules appear to be experimentally well-established for a wide variety of processes (see Reference 19):

$$G_M(Q^2) \sim (Q^2)^{-2}\,, \qquad F_\pi(Q^2) \sim (Q^2)^{-1} \tag{4.16}$$

and

$$\frac{d\sigma}{dt}\,(\gamma p \to \pi p) \sim (Q^2)^{-7}\,, \quad \frac{d\sigma}{dt}\,(\pi p \to \pi p) \sim (Q^2)^{-8}\,,$$
$$\frac{d\sigma}{dt}\,(pp \to pp) \sim (Q^2)^{-10}\,, \quad \frac{d\sigma}{dt}\,(\gamma p \to \gamma p)/\frac{d\sigma}{dt}\,(\gamma p \to \pi p) \sim Q^2 \tag{4.17}$$

at fixed $\theta_{c.m.}$.

(3) Since the distribution amplitudes ϕ_M and ϕ_B are $L_z = 0$ angular momentum projections of the hadronic wavefunctions, the sum of the quark spin along the hadron's momentum equals the hadron spin:[18]

$$\sum_{i \in H} S_i^z = S_H^z \,. \tag{4.18}$$

(In contrast in inclusive reactions there are any number of non-interacting quark and gluon spectators, so that the spin of the interacting constituents is only statistically related to the hadron spin — except possibly at the edge of phase-space $x \sim 1$.) Furthermore since all propagators in T_H are hard, the quark and hadron masses can be neglected at large Q^2 up to corrections of order $\sim m/Q$. The vector gluon interactions conserve quark helicity when all masses are neglected. Thus total quark helicity is conserved in T_H at large Q^2. Combining this with (4.18), we have the QCD selection rule:

$$\sum_{\text{initial}} \lambda_H = \sum_{\text{final}} \lambda_H \tag{4.19}$$

i.e., total hadron helicity is conserved up to corrections of order $O(m/Q)$.

Hadron helicity conservation thus applies for all large momentum transfer exclusive amplitudes involving light meson and baryons. Notice that the photon spin is not important: QCD predicts that $\gamma p \to \pi p$ is proton helicity conserving at fixed $\theta_{c.m.}$, $s \to \infty$, independent of the photon polarization. Exclusive amplitudes which involve hadrons with quarks or gluons in higher orbital angular momentum states are also suppressed by powers of the momentum transfer. An important corollary of this rule is that helicity-flip form factors are suppressed, e.g.:

$$F_2(Q^2)/F_1(Q^2) \sim O(m^2/Q^2) \quad . \tag{4.20}$$

The helicity rule, Eq. (4.19), is one of the most characteristic features of QCD, being a direct consequence of the gluon's spin. A scalar or tensor gluon-quark coupling flips the quark's helicity. Thus, for such theories, helicity may or may not be conserved in any given diagram contributing to T_H, depending upon the number of interactions involved. Only for a vector theory, like QCD, can we have a helicity selection rule valid to all orders in perturbation theory.

The study of timelike hadronic form factors using e^+e^- colliding beams can provide very sensitive tests of this rule, since the virtual photon in $e^+e^- \to \gamma^* \to h_A \bar{h}_B$ always has spin ± 1 along the beam axis at high energies. Angular momentum conservation implies that the virtual photon can "decay" with one of only two possible angular distributions in the center of momentum frame: $(1+\cos^2\theta)$ for $|\lambda_A - \lambda_B| = 1$, and $\sin^2\theta$ for $|\lambda_A - \lambda_B| = 0$ where $\lambda_{A,B}$ are the helicities of hadron $h_{A,B}$. Hadronic helicity conservation, Eq. (4.19), as required by QCD greatly restricts the possibilities. It implies that $\lambda_A + \lambda_B = 0$ (since the photon carries no "quark helicity"), or equivalently that $\lambda_A - \lambda_B = 2\lambda_A = -2\lambda_B$. Consequently, anguler momentum conservation requires $|\lambda_A| = |\lambda_B| = 1/2$ for baryons, and $|\lambda_A| = |\lambda_B| = 0$ for mesons; furthermore, the transfer distributions are now completely determined:

$$\frac{d\sigma}{d\cos\theta}(e^+e^- \to B\bar{B}) \propto 1+\cos^2\theta \quad \text{(baryons)} \tag{4.21}$$

$$\frac{d\sigma}{d\cos\theta}(e^+e^- \to M\bar{M}) \propto \sin^2\theta \quad \text{(mesons)} \tag{4.22}$$

We emphasize that these predictions are far from trivial for vector mesons and for all baryons. For example, one expects distributions like $1+\alpha\cos^2\theta$, $-1 < \alpha < 1$, in theories with a scalar or tensor gluon. So simply verifying these angular distributions would give strong evidence in favor of a vector gluon.

The power-law dependence in s of these cross sections is also predicted in QCD, using the dimensional counting rule. Such "all orders" predictions for QCD allowed processes are summarized in Table II. Processes suppressed in QCD are also listed there; these

Table II. Exclusive channels in e^+e^- annihilation. The $h_A\bar{h}_B\gamma^*$ couplings in allowed processes are $-ie(p_A - p_B)^\mu F(s)$ for mesons, $-ie\bar{v}(p_B)\gamma^\mu G(s)u(p_A)$ for baryons, and $-ie^2\varepsilon_{\mu\nu\rho\sigma}p_M^\nu\epsilon^\rho p_\gamma^\sigma F_{M\gamma}(s)$ for meson-photon final states. Similar predictions apply to decays of heavy-quark vector states, like the $\psi,\psi',\ldots$, produced in e^+e^- collisions.

	$e^+e^- \to h_A(\lambda_A)\bar{h}_B(\lambda_B)$	Angular distribution	$\sigma(e^+e^- \to h_A\bar{h}_B)/\sigma(e^+e^- \to \mu^+\mu^-)$
Allowed in QCD	$e^+e^- \to \pi^+\pi^-,\ K^+K^-$	$\sin^2\theta$	$\frac{1}{4}\lvert F(s)\rvert^2 \sim c/s^2$
	$\rho^+(0)\rho^-(0),\ K^{*+}K^{*-}$	$\sin^2\theta$	$\frac{1}{4}\lvert F(s)\rvert^2 \sim c/s^2$
	$\pi^o\gamma(\pm1),\eta\gamma,\eta'\gamma$	$1 + \cos^2\theta$	$(\pi\alpha/2)s\lvert F_{M\gamma}(s)\rvert^2 \sim c/s$
	$e^+e^- \to p(\pm\frac{1}{2})\bar{p}(\pm\frac{1}{2}),n\bar{n},\ldots$	$1 + \cos^2\theta$	$\lvert G(s)\rvert^2 \sim c/s^4$
	$p(\pm\frac{1}{2})\bar{\Delta}(\mp\frac{1}{2}),n\bar{\Delta},\ldots$	$1 + \cos^2\theta$	$\lvert G(s)\rvert^2 \sim c/s^4$
	$\Delta(\pm\frac{1}{2})\bar{\Delta}(\mp\frac{1}{2}),y^*\bar{y}^*,\ldots$	$1 + \cos^2\theta$	$\lvert G(s)\rvert^2 \sim c/s^4$
Suppressed in QCD	$e^+e^- \to \rho^+(0)\rho^-(\pm1),\pi^+\rho^-,K^+K^{*-},\ldots$	$1 + \cos^2\theta$	$< c/s^3$
	$\rho^+(\pm1)\rho^-(\pm1),\ldots$	$\sin^2\theta$	$< c/s^3$
	$e^+e^- \to p(\pm\frac{1}{2})\bar{p}(\pm\frac{1}{2}),p\bar{\Delta},\Delta\bar{\Delta},\ldots$	$\sin^2\theta$	$< c/s^5$
	$p(\pm\frac{1}{2})\bar{\Delta}(\pm\frac{3}{2}),\Delta\bar{\Delta},\ldots$	$1 + \cos^2\theta$	$< c/s^5$
	$\Delta(\pm\frac{3}{2})\bar{\Delta}(\pm\frac{3}{2}),\ldots$	$\sin^2\theta$	$< c/s^5$

all violate hadronic helicity conservation, and are suppressed by powers of m^2/s in QCD. This would not necessarily be the case in scalar or tensor theories.

The exclusive decays of heavy quark atoms $(\psi,\psi',\ldots)$ into light hadrons can also be analyzed in QCD.[18] The decay $\psi \to p\bar{p}$ for example proceeds via diagrams such as those in Fig. 2(b). Since ψ's produced in e^+e^- collisions must also have spin ± 1 along the beam direction and since they can only couple to light quarks via gluons, all the properties listed in Table II apply to ψ, ψ', T, T',... decays as well. There is considerable experimental data for the ψ and ψ' decays.[55]

Perhaps the most significant tests are the decays $\psi,\psi' \to p\bar{p},n\bar{n}$, ... The predicted angular distribution $1+\beta^2\cos^2\theta$ is consistent with published data.[35] This is important evidence favoring a vector gluon since scalar or tensor gluon theories would predict a distribution of $\sin^2\theta + O(\alpha_s)$. Dimensional counting rules can be checked by comparing the ψ and ψ' rates into $p\bar{p}$, normalized by the total rates into light-quark hadrons so as to remove dependence upon the heavy-quark wavefunctions. Theory predicts

$$\frac{BR(\psi \to p\bar{p})}{BR(\psi' \to p\bar{p})} \sim (M_{\psi'}/M_{\psi})^8 \tag{4.23}$$

where

$$BR(\psi \to p\bar{p}) \equiv \frac{\Gamma(\psi \to p\bar{p})}{\Gamma(\psi \to \text{light-quark hadrons})} \quad . \tag{4.24}$$

Existing data suggests a ratio $(M_{\psi'}/M_{\psi})^n$ with $n \sim 6 \pm 3$, in good agreement with QCD.

Many more examples of exclusive reactions which test the basic scaling laws and spin structure of QCD are discussed in References 18 and 19. The essential point is that exclusive reactions have the potential for isolating the QCD hard-scattering processes in situations where the helicities of all the interaction constituents are controlled. In contrast, in inclusive reactions the absence of restrictions on spectator quark and gluons allows only a statistical correlation between the constituent and hadronic helicities.

Two-Photon Processes[12]

One of the most important applications of perturbative QCD is to the two-photon processes $d\sigma/dt\ (\gamma\gamma \to M\bar{M})$, $M = \pi,\kappa,\rho,\omega$ at large $s = (k_1+k_2)^2$ and fixed $\theta_{c.m.}$. These reactions, which can be studied in $e^+e^- \to e^+e^-M\bar{M}$ processes, provide a particularly important laboratory for testing QCD since these "Compton" processes are, by far, the simplest calculable large-angle exclusive hadronic scattering reactions. As we discuss below, the large-momentum-transfer scaling

behavior, the helicity structure, and often even the absolute normalization can be rigorously computed for each two-photon channel.

Conversely, the angular dependence of the $\gamma\gamma \to M\bar{M}$ amplitudes can be used to determine the shape of the process-independent meson "distribution amplitudes," $\phi_M(x,Q)$, the basic short-distance wavefunctions which control the valence quark distributions in high momentum transfer exclusive reactions.

A critically important feature of the $\gamma\gamma \to M\bar{M}$ amplitude is that the contributions of Landshoff[17] pinch singularities are power-law suppressed at the Born level - even before taking into account Sudakov form factor suppression. There are also no anomalous contributions from the $x \sim 1$ endpoint integration region. Thus, as in the calculation of the meson form factors, each fixed-angle helicity amplitude can be written to leading order in $1/Q$ in the factorized form [$Q^2 = p_T^2 = tu/s$; $\tilde{Q}_x = \min(xQ,(1-x)Q)$] (See Fig. 9):

$$\mathcal{M}_{\gamma\gamma\to M\bar{M}} = \int_0^1 dx \int_0^1 dy\ \phi_{\bar{M}}(y,\tilde{Q}_y) T_H(x,y;s,\theta_{c.m.}) \phi_M(x,\tilde{Q}_x) \qquad (4.25)$$

where T_H is the hard-scattering amplitude $\gamma\gamma \to (q\bar{q})(q\bar{q})$ for the production of the valence quarks collinear with each meson and $\phi_M(x,Q)$ is the (process-independent) distribution amplitude for finding the valence q and $\bar{q}$ with light-cone fractions of the meson's momentum, integrated over transverse momenta $k_\perp < Q$. The contribution

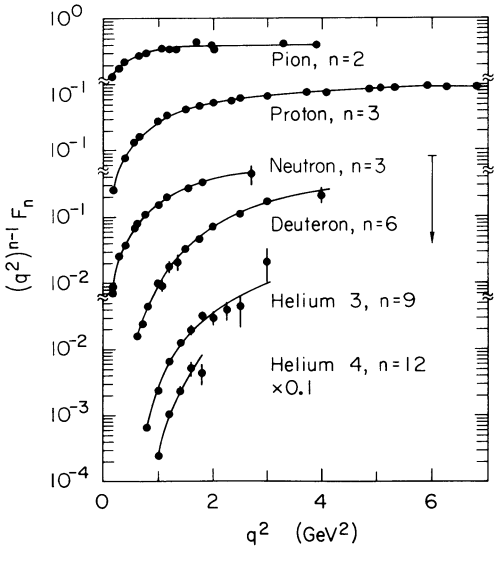

Fig. 9. Hadronic form factors multiplied by $(Q^2)^{n-1}$. (From Ref. 1).

of nonvalence Fock states are power-law suppressed. Further, the spin-selection rule (4.19) of QCD predicts that vector mesons M and $\bar{M}$ are produced with opposite helicities to leading order in 1/Q and all orders in $\alpha_s(Q^2)$.

Dimensional counting[8] predicts that for large s, $s^4\, d\sigma/dt$ scales at fixed t/s or $\theta_{c.m.}$ up to factors of $\ell n\, s/\Lambda^2$.

Some forty diagrams contribute to the hard-scattering amplitudes for $\gamma\gamma \to M\bar{M}$ (for nonsinglet mesons). These can be derived from the four independent diagrams in Fig. 10(b) by particle interchange. The resulting amplitudes for helicity zero mesons are:

$$\left.\begin{matrix} T_{++} \\ T_{--} \end{matrix}\right\} = \frac{16\pi\alpha_s}{3s}\,\frac{32\pi\alpha}{x(1-x)y(1-y)}\left(\frac{(e_1-e_2)^2 a}{1-\cos^2\theta_{c.m.}}\right) \tag{4.26}$$

$$\left.\begin{matrix} T_{++} \\ T_{--} \end{matrix}\right\} = \frac{16\pi\alpha_s}{3s}\,\frac{32\pi\alpha}{x(1-x)y(1-y)}\left(\frac{(e_1-e_2)^2(1-a)}{1-\cos^2\theta_{c.m.}} + \frac{e_1 e_2 a(y(1-y)+x(1-x))}{a^2-b^2\cos^2\theta_{c.m.}}\right) \tag{4.27}$$

where $\left.\begin{matrix} a \\ b \end{matrix}\right\} = (1-x)(1-y) \pm xy$, the subscripts ++, --, ... refer to photon helicities, and e_1, e_2 are the quark charges [i.e., the mesons have charges $\pm(e_1-e_2)$]. To compute the $\gamma\gamma \to M\bar{M}$ amplitude $\mathcal{M}_{\lambda\lambda}$, Eq.(4.25)], we now need only know the x-dependence of the meson's distribution

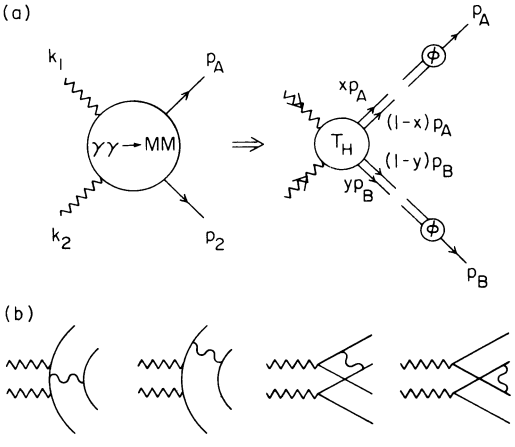

Fig. 10. (a) Factorized structure of the $\gamma\gamma \to M\bar{M}$ amplitude in QCD at large momentum transfer. The T_H amplitude is computed with quarks collinear with the outgoing mesons. (b) Diagram contributing to $T_H(\gamma\gamma \to M\bar{M})$ to lowest order in α_s.

amplitude $\phi_M(x,\tilde{Q})$; the overall normalization of ϕ_M is fixed by the 'sum rule' ($n_c = 3$)

$$\int_0^1 dx\ \phi_M(x,Q) = \frac{f_M}{2\sqrt{3}} \tag{4.28}$$

where f_M is the meson decay constant as determined from leptonic decays. Note that the dependence in x and y of several terms in $T_{\lambda\lambda'}$, is quite similar to that appearing in the meson's electromagnetic form factor (3.23):

$$F_M(s) = \frac{16\pi\alpha_s}{3s} \int_0^1 dx\ dy\ \frac{\phi_M^*(x,\tilde{Q}_x)\phi_M^*(y,\tilde{Q}_y)}{x(1-x)y(1-y)} \tag{4.29}$$

where $\phi_M(x,Q) = \phi_M(1-x,Q)$ is assumed. Thus much of the dependence on $\phi(x,Q)$ can be removed from $\mathcal{M}_{\lambda\lambda'}$, by expressing it in terms of the meson form factor — i.e.,

$$\left.\begin{matrix}\mathcal{M}_{++}\\ \mathcal{M}_{--}\end{matrix}\right\} = 16\pi\alpha\ F_M(s) \left(\frac{\langle(e_1-e_2)^2\rangle}{1-\cos^2\theta_{c.m.}}\right) \tag{4.30}$$

$$\left.\begin{matrix}\mathcal{M}_{+-}\\ \mathcal{M}_{-+}\end{matrix}\right\} = 16\pi\alpha\ F_M(s) \left(\frac{\langle(e_1-e_2)^2\rangle}{1-\cos^2\theta_{c.m.}}\right) + 2\langle e_1e_2\rangle g\left(\theta_{c.m.};\phi_M\right) \tag{4.31}$$

up to corrections of order α_s and m^2/s. Now the only dependence on ϕ_M, and indeed the only unknown quantity, is in the θ-dependent factor

$$g[\theta_{c.m.};\phi_M] = \frac{\int_0^1 dx\,dy\ \frac{\phi_M^*(x,\tilde{Q})\phi_M^*(y,\tilde{Q})}{x(1-x)\,y(1-y)}\ \frac{a[y(1-y)+x(1-x)]}{a^2-b^2\cos^2\theta_{c.m.}}}{\int_0^1 dx\,dy\ \frac{\phi_M^*(x,\tilde{Q})\phi_M^*(y,\tilde{Q})}{x(1-x)y(1-y)}} . \tag{4.32}$$

The spin-averaged cross section follows immediately from these expressions:

$$\frac{d\sigma}{dt} = \frac{2}{s}\ \frac{d\sigma}{d\cos\theta_{c.m.}} = \frac{1}{16\pi s^2}\ \frac{1}{4}\ \sum_{\lambda\lambda'} |\mathcal{M}_{\lambda\lambda'}|^2$$

$$= 16\pi\alpha^2 \left|\frac{F_M(s)}{s}\right|^2 \left\{ \frac{\langle(e_1-e_2)^2\rangle^2}{(1-\cos^2\theta_{c.m.})^2} + \frac{2\langle e_1e_2\rangle\langle(e_1-e_2)^2\rangle}{1-\cos^2\theta_{c.m.}} \right.$$

$$\left. \times g[\theta_{c.m.};\phi_M] + 2\langle e_1e_2\rangle^2 g^2[\theta_{c.m.};\phi_M] \right\} . \tag{4.33}$$

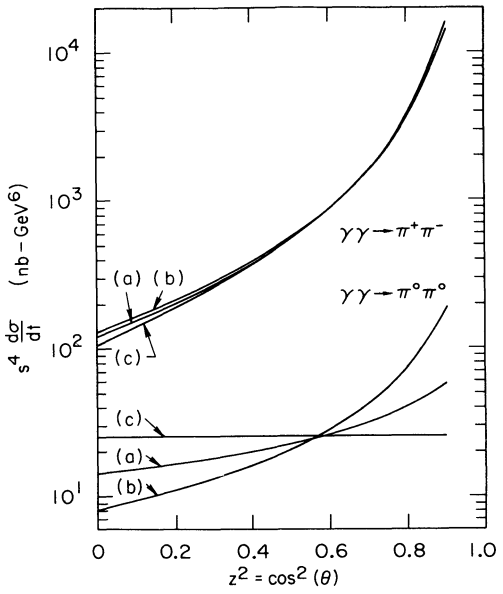

Fig. 11. QCD predictions for $\gamma\gamma \to \pi\pi$ to leading order in QCD. The results assume the pion form factor parametrization $F_\pi(s) \sim 0.4$ GeV^2/s. Curves (a), (b) and (c) correspond to the distribution amplitudes $\phi_M = x(1-x)$, $[x(1-x)]^{\frac{1}{4}}$, and $\delta(x-\frac{1}{2})$, respectively. Predictions for other helicity zero mesons are obtained by multiplying with the scale constants given in Ref. 15.

In Fig. 11 the spin-averaged cross section (for $\gamma\gamma \to \pi\pi$) are plotted for several forms of $\phi_M(x,Q)$. At very large energies, the distribution amplitude evolves to the form

$$\phi_M(x,Q) \xrightarrow[Q\to\infty]{} \sqrt{3}\, f_M\, x(1-x) \ , \tag{4.34}$$

and the predictions [curve (a)] become exact and parameter-free. However this evolution with increasing Q^2 is very slow (logarithmic), and at current energies ϕ_M could be quite different in structure, depending upon the details of hadronic binding. Curves (b) and (c) correspond to the extreme examples $\phi_M \propto [x(1-x)]^{\frac{1}{4}}$ and $\phi_M \propto \delta(x-\frac{1}{2})$, respectively. Remarkably, the cross section for charged mesons is essentially independent of the choice of ϕ_M, making this an essentially parameter-free prediction of perturbative QCD. By contrast, the predictions for neutral helicity-zero mesons are quite sensitive to the structure of ϕ_M. Thus we can study the x-dependence of the meson distribution amplitude by measuring the angular dependence of this process.

The cross sections shown in Fig. 8 are specifically for $\gamma\gamma \to \pi\pi$, where the pion form factor has been approximated by $F_\pi(s) \sim 0.4\ \text{GeV}^2/s$. The $\pi^+\pi^-$ cross section is quite large at moderate s:

$$\frac{\frac{d\sigma}{dt}(\gamma\gamma \to \pi^+\pi^-)}{\frac{d\sigma}{dt}(\gamma\gamma \to \mu^+\mu^-)} \sim \frac{4|F_\pi(s)|^2}{1-\cos^4\theta_{c.m.}}$$

$$\sim \frac{0.6\ \text{GeV}^4}{s^2} \qquad \text{at} \qquad \theta_{c.m.} = \pi/2 \ . \tag{4.35}$$

Similar predictions are possible for other helicity-zero mesons. The normalization of $\gamma\gamma \to M\bar{M}$ relative to the $\gamma\gamma \to \pi\pi$ cross section is completely determined by the ratio of meson decay constants $(f_M/f_\pi)^4$ and by the flavor-symmetry of the wavefunctions, provided only that ϕ_M and ϕ_π are similar in shape. Note that the cross section for charged ρ's with helicity zero is almost an order of magnitude larger than that for charged π's.

Finally notice that the leading order predictions [Eq.(4.33)] have no explicit dependence on α_s. Thus they are relatively insensitive to the choice of renormalization scheme or of a normalization scale. This is not the case for either the form factor or the two-photon annihilation amplitude when examined separately. However by combining the two analyses as in Eq. (4.33) we obtain meaningful results without computing $O(\alpha_s)$ corrections. The corresponding calculations for helicity-one mesons are given in Reference 12. Hadronic helicity conservation implies that only helicity-zero mesons can couple to a single highly virtual photon. So $F_{M_\perp}$, the transverse form factor cannot be measured experimentally. For simplicity we will assume that the longitudinal and transverse form factors are equal to obtain a rough estimate of the $\gamma\gamma \to \rho_\perp\rho_\perp$ cross section (Fig. 12). Again we see strong dependence on $\phi_{M_\perp}$ for all angles except $\theta_{c.m.} \sim \pi/2$, where the terms involving $g_\perp$ vanish. Consequently a measurement of the angular distribution would be very sensitive to the x-dependence of $\phi_{M_\perp}$, while measurements at $\theta_{c.m.} = \pi/2$ determine $F_{M_\perp}(s)$. Notice also that the number of charged ρ-pairs (with any helicity) is much larger than the number of neutral ρ's, particularly near $\theta_{c.m.} = \pi/2$. The cross sections are again quite large with

$$\left.\frac{\frac{d\sigma}{dt}(\gamma\gamma \to \rho_\perp^+\rho_\perp^-)}{\frac{d\sigma}{dt}(\gamma\gamma \to \mu^+\mu^-)}\right|_{\theta_{c.m.}=\pi/2} \sim \frac{5\ \text{GeV}^4}{s^2} \ . \tag{4.36}$$

Results for other mesons are given in Reference 12.

The $\gamma\gamma \to M\bar{M}$ and $\gamma^*\gamma \to M$ processes thus provide detailed checks of the basic Born structure of QCD, the scaling behavior of the

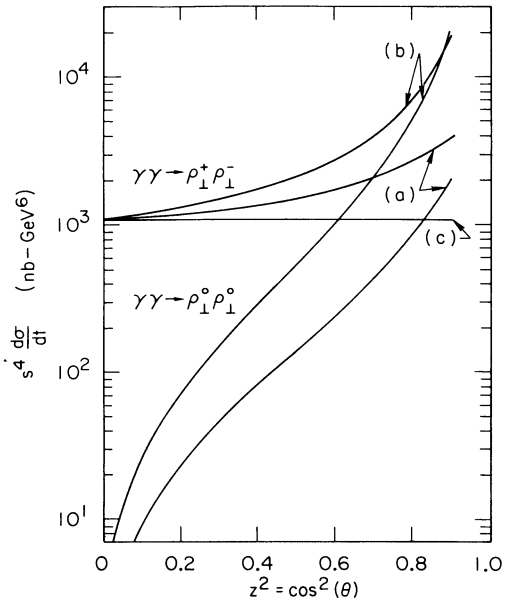

Fig. 12. QCD predictions for $\gamma\gamma \to \rho_\perp \bar{\rho}_\perp$ with opposite helicity ± 1 to leading order in QCD. The normalization given here assumes that the ρ distribution amplitude is helicity independent.

quark and gluon propagators and interactions, as well as the contituent charges and spins. Conversely, the angular dependence of the $\gamma\gamma \to M\bar{M}$ amplitudes can be used to determine the shape of the process-independent distribution amplitude $\phi_M(x,Q)$ for valence quarks in the meson $q\bar{q}$ Fock state. The $\cos\theta_{c.m.}$-dependence of the $\gamma\gamma \to M\bar{M}$ amplitude determines the light-cone x-dependence of the meson distribution amplitude in much the same way that the x_{Bj} dependence of deep inelastic cross sections determines the light-cone x-dependence of the structure functions (quark probability functions) $G_{q/M}(x,Q)$.

The form of the predictions given here are exact to leading order in $\alpha_s(Q^2)$. Power-law $(m/Q)^2$ corrections can arise from mass insertions, higher Fock states, pinch singularities and nonperturbative effects. In particular, the predictions are only valid when s-channel resonance effects can be neglected. It is likely that the background due to resonances can be reduced relative to the leading order QCD contributions if one measures the two-photon processes with at least one of the photons tagged at moderate space-like momentum q^2, since resonance contributions are expected to be strongly damped by form factor effects. In contrast, the leading order QCD $\gamma_1\gamma_2 \to M\bar{M}$ amplitudes are relatively insensitive to the value of q_1^2 or q_2^2 for $|q_i^2| \ll s$.

Finally, we note that the amplitudes given above have simple crossing properties. In particular, we can immediately analyze the Compton amplitude $\gamma M \to \gamma M$ in the region t large enough with $s >> |t|$ in order to study the leading Regge behavior in the large momentum transfer domain. In the case of helicity ± 1 mesons, the leading contribution to the Compton amplitude has the form ($s >> |t|$)

$$\mathcal{M}_{\gamma M \to \gamma M} = 16\pi\alpha \; F_{M_\perp}(t)(e_1^2 + e_2^2) ; \quad (\lambda_\gamma = \lambda'_\gamma , \quad \lambda_M = \lambda'_M) \tag{4.37}$$

which corresponds to a fixed Regge singularity at $J = 0$.[56] In the case of helicity zero mesons, this singularity actually decouples, and the leading J-plane singularity is at $J = -2$.

V. DEEP INELASTIC LEPTON SCATTERING

The crucial evidence that the electromagnetic current within hadrons is carried by point-like spin 1/2 quarks comes from deep-inelastic electron, muon and neutrino scattering. At large momentum transfer, $Q^2 \lesssim 2$ GeV^2 the lepton-nucleon inelastic cross section displays a scale-invariant behavior consistent with the simplest type of impulse approximation — where the electron scatters directly against point-like quark constituents of the target.[57] The deviations which are observed at very large Q^2 are consistent with the color radiative corrections predicted by QCD. In addition at low values of Q^2, there is evidence for power-law "high twist" corrections associated with coherent multiquark processes, interference effects, and final state corrections — quite in analogy to the corrections to impulse approximation expected in nuclear physics inelastic breakup calculations.

The Fock state representation we discussed in Section III provides a particularly simple and elegant basis for calculating the deep inelastic cross section in QCD. We first consider the forward Compton amplitude $\gamma^* p \to \gamma^* p$ with virtual photon mass $q^2 = -Q^2 < 0$, and then calculate the $ep \to eX$ cross section from the absorptive part. An ideal Lorentz frame is

$$p = (p^+, p^-, \vec{p}_\perp) = (p^+, \frac{M^2}{p^+}, \vec{0}_\perp) \tag{5.1}$$

$$q = (q^+, q^-, \vec{q}_\perp) = (0 , \frac{2p\cdot q}{p^+}, \vec{q}_\perp) \tag{5.2}$$

with $q^2 = Q^2$ and $p\cdot q = M\nu$. For the diagram 13(b) which has no final state interactions, the (light-cone) energy denominator between the photon interaction is

$$D = M^2 + 2M\nu - \frac{(\vec{k}_\perp + \vec{q}_\perp)^2 + m^2}{x} - \sum_{i \neq 1} \left(\frac{k_\perp^2 + m^2}{x}\right)_i + i\varepsilon \tag{5.3}$$

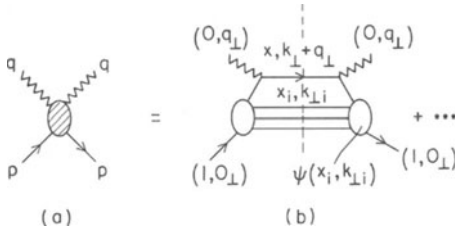

Fig. 13. Calculation of the forward virtual Compton amplitude. Diagram (b) gives the impulse approximation, neglecting final state and multiquark interactions.

where m is the struck quark mass, and the sum over $i \neq 1$ gives the spectator quark and gluon contributions. For states with $|\mathcal{E}| = |M^2 - \sum_i (k_\perp^2 + m^2)/x| \ll 2M\nu$ and $k_\perp^2 \ll Q^2$ we can write

$$D \cong 2M\nu - \frac{Q^2}{x} + i\varepsilon \tag{5.4}$$

$$\text{Im } D^{-1} = \frac{x\pi}{2M\nu}\,\delta\left(x - \frac{Q^2}{2M\nu}\right) \tag{5.5}$$

i.e., the electron scattering on a quark with light-cone momentum fraction

$$x \equiv \frac{k^o + k^3}{p^o + p^3} \cong \frac{Q^2}{2M\nu} = x_{Bj} \quad . \tag{5.6}$$

The corresponding impulse approximation cross section is $(x \to x_{Bj})$

$$\frac{d\sigma}{dQ^2\,dx}(\ell p \to \ell' X) = \sum_q G_{q/p}(x,a)\,\frac{d\sigma}{dQ^2}(\ell q \to \ell' q)\Big|_{p_q = xp} \tag{5.7}$$

where[21]

$$G_{q/p}(x,Q) = \sum_{n\geq 3} \int^Q [d^2k_\perp][dx]\,|\psi_n^Q(x,k_\perp)|^2\,\delta(x - x_q) \tag{5.8}$$

gives the probability distribution for finding the quark with fractional light-cone momentum collinear up to the scale $k_\perp^2 < Q^2$, $|\mathcal{E}| < 2M\nu$. Unlike large momentum transfer exclusive amplitudes, all Fock states contribute to the inclusive cross section. The subprocess cross section $d\sigma/dQ^2(\ell q \to \ell' q)$ is evaluated for a quark collinear with the proton momentum $p_q^+ = xp^+$, $\vec{k}_\perp \simeq 0$. Since all the loop corrections to the subprocess cross section are hard ($k_\perp \gtrsim 0(Q^2)$), it can be developed as a power series in $\alpha_s(Q^2)$. Thus the only correction to perfect scale invariance of $d\sigma/dx\,dQ^2$ at large Q^2 and

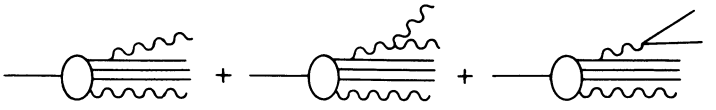

Fig. 14. Contributions to the hadron Fock state wavefunction which give $\psi \sim 1/k_\perp$ at large $k_\perp$ and thus structure function evolution.

fixed x_{Bj} comes for the Q^2 dependence of the probability distribution $G(x,Q^2)$. This in turn can only arise from the wavefunction renormalization or from contributions $\psi_n \sim O(1/k_\perp)$ at large $k_\perp$. In QCD these occur only from the perturbative processes $q \to qg$ and $g \to gg$, $g \to q\bar{q}$, as illustrated in Fig. 14. In parallel to the derivation of the evolution equation for the distribution amplitude, we then can derive evolution equations for the distributions $G_{q/H}(x,Q^2)$ and $G_{g/H}(x,Q^2)$ of the form[58,59]

$$\frac{\partial}{\partial \log Q^2} G(x,Q) = \frac{\alpha_s(Q^2)}{2\pi} \int_x^1 P\left(\frac{x}{y}\right) G(y,Q) \frac{dy}{y} \quad . \tag{5.9}$$

For example, for the "non-singlet" distribution

$$G_{q/H}(x,Q) = G_{q/H}(x,Q) - G_{\bar{q}/H}(x,Q) \tag{5.10}$$

we have to lowest order in $\alpha_s(Q^2)$, $(C_F = 4/3)$

$$P_{q/q}(z) = C_F\left(\frac{1+z^2}{1-z}\right)_+ = C_F\left[\frac{1+z^2}{1-z} - \delta(1-z)\int_0^1 dx\, \frac{1+x^2}{1-x}\right] \quad . \tag{5.11}$$

(The subtraction term, which ensures finite behavior at $x_g = 0$, arises from the wavefunction renormalization, as in Eq. (3.14)). The Q^2 dependence can be displayed most simply by taking moments:

$$M_n(Q^2) = \int_0^1 G(x,Q^2)\, x^n dx \quad . \tag{5.12}$$

Then

$$M_n^{NS} = M_n^{NS}(Q_o^2) \left(\frac{\log Q^2/\Lambda^2}{\log Q_o^2/\Lambda^2}\right)^{-\gamma_n} \tag{5.13}$$

where the γ_n are defined in Eq. (3.16). The higher order corrections to the Q^2-evolution of M_n are discussed in References 1 and 2. A critical feature[21] is the fact that the higher loop

corrections (e.g., from the higher Fock states) are constrained kinematically to $k_\perp^2 < (1-y)Q^2 < (1-x)Q^2$, where y is labelled in the figure; i.e., the evolution is reduced at large x and for large n. A detailed discussion is given in Reference 41.

Equation (5.7) displays an essential feature of the QCD predictions for inclusive reactions: the factorization of the physical cross section into a hard-scattering subprocess cross section, controlled by short-distance perturbative QCD, convoluted with structure functions $G(x,Q^2)$ which contain the long distance hadronic bound state dynamics. Notice that the Q^2-evolution of $G(x,Q)$ is also completely specified by the perturbative QCD processes and is independent of the nature of the target.

All the corrections to the perturbative QCD impulse approximation from final state interactions, finite $k_\perp^2$ effects, interference contributions, mass corrections, etc. are of higher order in $1/Q^2$, at least when analyzed using perturbative methods. In the operator product analysis these contributions correspond to matrix elements of "higher twist" operators which have non-minimal dimensions. The most important higher twist terms for deep inelastic lepton scattering are expected to correspond to processes where the lepton scatters on multiparticle clusters in the target (qq, $q\bar{q}$, virtual mesons, qg, etc.). We thus obtain a sum of contributions (see Fig. 15):[15]

$$\frac{d\sigma}{dQ^2 dx}(\ell H \to \ell' X) = \sum_{a \in H} G_{a/H}(x) \frac{d\sigma}{dQ^2}(ea \to ea)\Big|_{p_a = xp_H} \tag{5.14}$$

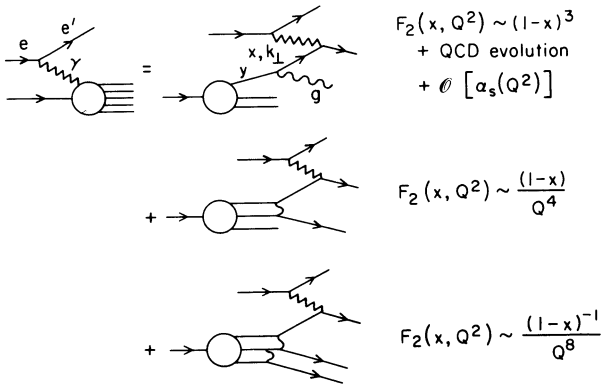

Fig. 15. QCD contributions to inelastic electron-nucleon scattering, including radiative and higher twist (diquark, triquark) corrections.

where, in general, $d\sigma_a/dQ^2$ falls in Q^2 according to the compositeness of a:

$$\frac{d\sigma}{dQ^2}(\ell a \to \ell' a) \sim \frac{4\pi\alpha^2}{Q^4} |F_a(Q^2)|^2 \quad . \tag{5.15}$$

For example, the "diquark" eqq $\to$ eqq gives a contribution to ep $\to$ eX of relative order $(m^2/Q^2)^2$. Since the qq can carry a large fraction of the proton's momentum, this contribution can be significant at large x. For a guide to this effect one can use the spectator counting rule:[60,8]

$$G_{a/H}(x) \underset{x\to 1}{\sim} (1-x)^{2n_s-1} \tag{5.16}$$

where n_s is the minimum number of spectator quarks (or gluons) in the Fock state required to stop at $x \to 1$. The minimal Fock state containing a gives the dominant contribution.

The simplified rule (5.16) can be derived from minimally connected tree graph diagrams, ignoring spin effects, or from simple phase space considerations if one ignores the spectator quark masses[61] (see Section VI). Using this simple counting we can then classify the contributions to the hadron structure functions, as illustrated in Fig. 15. The diquark contribution is expected to give a large contribution to the longitudinal structure function since it acts coherently as a boson current. The order $\alpha_s(Q^2)$ contribution from the hard gluon radiative corrections with $k_\perp^2 > (1-x)Q^2$ also gives a significant contribution to σ_L.

A detailed derivation of the behavior of structure functions at $x \sim 1$ from perturbative QCD is given in Reference 21. At $x \sim 1$ all of the hadron's momentum must be carried by one quark, and each quark and gluon quark and gluon propagator which transfers this momentum becomes far off shell:

$$k^2 \sim O\left(-\frac{k_\perp^2 + m^2}{1-x}\right) \quad .$$

Perturbative QCD predictions thus become relevant. An important result is that at large x the struck quark tends to have the same helicity as the target nucleon:[21,62]

$$G_{q\uparrow/p\uparrow} \sim (1-x)^3 \; ; \qquad G_{q\downarrow/p\uparrow} \sim (1-x)^5 \quad . \tag{5.17}$$

This type of spin correlation is consistent with the SLAC-Yale polarized electron/polarized target data. Combined with the SU(6) symmetry of the nucleon wavefunction of this implies that the leading quark in the proton is five times more likely to be an up quark than a down quark, and thus[62] $(F_2 = \sum_q e_q^2 \, x G_{q/n})$

$$F_{2n}(x,Q^2)/F_{2p}(x,Q^2) \xrightarrow[x\sim 1]{} 3/7 \quad . \tag{5.18}$$

For the case of mesons, the perturbative QCD gluon exchange prediction is[63]

$$G_{q/m} \sim (1-x)^2 \quad . \tag{5.19}$$

In addition, the same QCD analysis predicts a large C/Q^2 contribution to the meson longitudinal structure function (see Fig.3(b)):[22,64]

$$F_L^{\pi}(x,Q^2) = \frac{2x^2}{Q^2} C_F \int_{\sim m^2/(1-x)}^{Q^2} dk^2 \, \alpha_s(k^2) \, F_{\pi}(k^2) \tag{5.20}$$

which numerically is $F_L \sim x^2/Q^2$ in GeV^2 units. This contribution, which can dominate leading twist quark distributions in mesons is normalized in terms of the meson distribution amplitude, which in turn is normalized by the pion form factor.

The dominance of the longitudinal structure functions in the fixed W limit for mesons is an essential prediction of perturbative QCD. Perhaps the most dramatic consequence is in the Drell-Yan process $\pi p \to \ell^+\ell^- X$; one predicts[22] that for fixed pair mass Q, the angular distribution of the ℓ^+ (in the pair rest frame) will change from the conventional $(1+\cos^2\theta_+)$ distribution to $\sin^2(\theta_+)$ for pairs produced at large x_L. A recent analysis of the Chicago-Illinois-Princeton experiment[65] at FNAL appears to confirm the QCD high twist prediction with about the expected normalization. Striking evidence for the effect has also been seen in a Gargamelle analysis[66] of the quark fragmentation functions in $\nu p \to \pi^+ \mu^- X$. The results yield a quark fragmentation distribution into positive charged hadrons which is consistent with the predicted form: $dN^+/dzdy \sim B(1-z)^2 + (C/Q^2)(1-y)$ where the $(1-y)$ behavior corresponds to a longitudinal structure function. It is also crucial to check that the $e^+e^- \to MX$ cross section becomes purely longitudinal $(\sin^2\theta)$ at large z at moderate Q^2.[62]

The results (5.17) and (5.19) for $G_{q/B}$ and $G_{q/M}$ give the behavior of the leading QCD contribution to the structure function before QCD evolution is applied; e.g., the results are valid for $F_2(x,Q^2)$ at Q^2 of order of $\langle k_\perp^2 \rangle_H$. The large Q^2 behavior is determined by the evolution equation (5.9), taking account of the phase space limits of the radiated gluons at $x \sim 1$.[41]

VI. THE PHENOMENOLOGY OF HADRONIC WAVEFUNCTIONS

Thus far, most of the phenomenological tests of QCD have focused on the dynamics of quark and gluon subprocesses in inclusive

high momentum transfer reactions. The Fock state wavefunctions $\psi_n^{\kappa}(x_i,\vec{k}_{\perp i};\lambda_i)$ which determine the dynamics of hadrons in terms of their quark and gluon degrees of freedom are also of fundamental importance. If these wavefunctions were accurately known then an extraordinary number of phenomena, including decay amplitudes, exclusive processes, higher twist contributions to inclusive phenomena, structure functions, and low transverse momentum phenomena (such as diffractive processes, leading particle production in hadron-hadron collisions and heavy flavor hadron production) could be interrelated. Conversely, these processes can provide phenomenological constraints on the Fock state wavefunctions which are important for understanding the dynamics of hadrons in QCD. In addition, as we discuss in Reference 67, the structure of nuclear wavefunctions in QCD is essential for understanding the syntheses of nuclear physics phenomenology with QCD.

A. Measures of Hadron Wavefunctions

As we have shown in Section III the central measures of the hadron wavefunctions are the distribution amplitudes

$$\phi(x_i,Q) = \int^{Q} [d^2k_\perp]\ \psi^{Q}_{val}(x_i,\vec{k}_{\perp i}) \tag{6.1}$$

which control high momentum transfer form factors and exclusive processes:

$$\mathcal{M} \cong \Pi\ \phi \otimes T_H \tag{6.2}$$

and the quark and gluon structure functions

$$G_{q/H}(x,Q) = \sum_n \int^{Q} [d^2k_\perp][dx]\,|\psi_n(x_i,k_{\perp i})|^2\,\delta(x-x_q) \tag{6.3}$$

which control high momentum transfer inclusive reactions

$$d\sigma \cong \Pi\ G \otimes d\hat{\sigma} \tag{6.4}$$

Examples are shown in Figs. 1 through 3. A summary of the basic properties, logarithmic evolution, and power-law behavior of these quantities is given in Table III.

The exclusive formula (6.2) also includes applications to large momentum transfer multiparticle production[68,8] $e^+e^- \to H_1 \ldots H_n$ with $p_i \cdot p_j \sim O(Q^2)$, and the elastic and inelastic weak and electromagnetic form factors. We also note that hard scattering higher twist subprocesses to inclusive reactions such as $\gamma q \to Mq$, $gq \to Mq$, $q\bar{q} \to M\bar{M}$, $qq \to B\bar{q}$, etc. are absolutely normalized in terms of the distributions amplitudes.[69] In particular, some amplitudes such

Table III. Comparison of exclusive and inclusive cross sections.

Exclusive amplitudes	Inclusive cross sections
$\mathcal{M} \sim \Pi \phi(x_i,Q) \otimes T_H(x_i,Q)$	$d\sigma \sim \Pi G(x_a,Q) \otimes d\hat{\sigma}(x_a,Q)$
$\phi(x,Q) = \int^Q [d^2k_\perp] \psi^Q_{val}(x,k_\perp)$	$G(x,Q) = \sum_n \int^Q d^2k_\perp [dx]' \lvert\psi_n(x,k_\perp)\rvert^2$
Measure ϕ in $\gamma\gamma \to M\bar{M}$	Measure G in $\ell p \to \ell X$
$\sum_{i\in H} \lambda_i = \lambda_H$	$\sum_{i\in H} \lambda_i \neq \lambda_H$

EVOLUTION

$\frac{\partial\phi(x,Q)}{\partial \log Q^2} = \alpha_s \int [dy] V(x,y)\phi(y)$	$\frac{\partial G(x,Q)}{\partial \log Q^2} = \alpha_s \int dy\ P(x/y)G(y)$
$\lim_{Q\to\infty} \phi(x,Q) = \Pi_i x_i \cdot C_{flavor}$	$\lim_{Q\to\infty} G(x,Q) = \delta(x)\ C'$

POWER LAW BEHAVIOR

$\frac{d\sigma}{dx}(A+B \to C+D) \cong \frac{1}{s^{n-2}} f(\theta_{CM})$	$\frac{d\sigma}{d^2p/E}(AB \to CX) \cong \frac{(1-x_T)^{2n_s-1}}{(Q^2)^{n_{act}-2}} f(\theta_{CM})$
$n = n_A + n_B + n_C + n_D$	$n_{act} = n_a + n_b + n_c + n_d$
T_H: expansion in $\alpha_s(Q^2)$	$d\hat{\sigma}$: expansion in $\alpha_s(Q^2)$

COMPLICATIONS

End point singularities	Multiple scales
Pinch singularities	Phase-space limits on evolution
Higher Fock states	Heavy quark thresholds
	Higher twist multiparticle processes
	Initial and final state interactions

as $\gamma q \to \pi q$, $q\bar{q} \to \pi g$ and $gq \to \pi q$ can be rigorously related to the pion form factor since the same integral

$$\int_0^1 \frac{dx}{1-x}\, \phi_\pi(x,Q) \tag{6.5}$$

enters in each of the quantities.[70] The p_T^{-6} processes[24] $gq \to Mq$ (see Fig. 3(a)) and $q\bar{q} \to Mq$ are particularly interesting and important in high-p_T meson production processes such as $pp \to MX$ since the meson is produced directly in the subprocess without the necessity for quark or gluon jet fragmentation. In fact the contributions of standard p_T^{-4} scaling processes such as $qq \to qq$, $gq \to gq$, and $gg \to gg$ are strongly suppressed by two to three orders of magnitude relative to the "directly coupled" contributions because of the suppression of jet fragmentation $D_{M/q}(z)$ at large momentum fraction z and the fact that the subprocesses must occur at a significantly larger momentum transfer than that of the triggered particle.[71]

Despite much effort there is at this time no systematic understanding of high p_T hadron production in QCD. A comprehensive attack must take into account not only leading twist subprocesses and directly coupled higher twist contributions such as those listed above, but also the effects of initial state multiple scattering effects. One of the most important experiments which could clarify the nature of these effects is the measurement of the ratio of direct photon to meson at high p_T: $(x_T = 2p_T/\sqrt{s})$

$$R_{\gamma/\pi}(x_T, s, \theta_{cm}) = \frac{d\sigma}{d^3p/E}(pp \to \gamma X) \Big/ \frac{d\sigma}{d^3p/E}(pp \to \pi X) \ . \tag{6.6}$$

For example, if leading twist QCD processes dominate these reactions then $R_{\gamma/\pi} \sim f(x_T) \sim (1-x_T)^{-2}$ at $\theta_{cm} \sim \pi/2$. If directly-coupled processes such as $gq \to \pi q$ dominate the meson production then one predicts $R_{\gamma/\pi} \sim p_T^2$ at fixed x_T and θ_{cm}.[72] Measurements of this ratio in nuclear targets is important for clarifying the contribution of final state multiple scattering processes.

The photon probe plays a crucial role in high-p_T hadron reactions since the photon couples directly to the quark and gluon subprocesses at short distances. The most dramatic example of these point-like phenomena is the recent observations at PETRA[6-8] of high transverse momentum hadrons in $\gamma\gamma$ collisions. The results at $p_T \geq 3$ GeV appear to be consistent with the scale invariant QCD prediction[73]

$$\frac{d\sigma(\gamma\gamma \to \text{jet} + \text{jet})}{d\sigma(\gamma\gamma \to \mu^+\mu^-)} = 3 \sum_{q=u,d,s,c} e_q^4 \left[1 + 0\left(\frac{\alpha_s(p_T^2)}{\pi}\right)\right] , \tag{6.7}$$

These results also indicate that, unlike typical meson-induced reactions, an incident photon often produces high p_T hadronic jets without leaving hadronic energy in the beam fragmentation direction.[74] One also expects analogous results for directly coupled photons in $\gamma p \to HX$ and $\gamma p \to Jet + X$ reactions. The point-like behavior of on-shell photons is in direct contrast to the predictions of vector meson dominance models.

A surprising feature of QCD is that even a hadron can produce jets at large p_T without beam fragmentation.[70] For example, the existence of high twist subprocesses such as $Mq \to gq$ and $Mg \to q\bar{q}$ leads to high p_T jet events in meson-induced collisions $Mp \to Jet + Jet + X$ where there is no hadronic energy left in the meson beam fragmentation direction (see Fig. 3(c)). The inclusive cross section, which scales as p_T^{-6} at fixed x_T and θ_{cm}, is absolutely normalized to the meson form factor. As in the case of the photon-induced reactions the directly coupled meson has no associated color radiation or structure function evolution. An experimental search for these unique and highly kinematically constrained events is very important in order to confirm the presence of these subprocesses which involve the direct coupling of meson $q\bar{q}$ Fock state to quarks and gluons at short distance.

In general, we can replace any direct photon interaction by a direct-coupled meson interaction in the subprocess cross section by the replacement $\alpha \gtrsim F_\pi(p_T^2)$. Furthermore, one can compute direct-coupled processes which isolate the valence Fock state of baryons, e.g., $pp \to pX$ (production of isolated large p_T protons via the $qq \to p\bar{q}$ subprocesses), and reactions $pp \to qqX$ (from $\bar{q}p \to qq$) (see Fig. 3(d)), $pp \to qqqX$ (from $gp \to qqq$) etc., each of which produce jets at high p_T without beam spectators or fragmentation.

B. Constraints on the Pion and Proton Valence Wavefunction[27]

The central unknown in the QCD analysis of hadronic matrix elements is the hadron wavefunction in the non-perturbative domain $\kappa^2 \lesssim 1\ GeV^2$. For illustration we shall assume that in this region the ψ_n fall off exponentially in the off-shell energy:

$$\psi_n^\kappa(x_i, k_{\perp i}) = A_n\, e^{b_n^2 \mathcal{E}_n} \tag{6.8}$$

$$\mathcal{E}_n = M^2 - \sum_{i=1}^{n} \left(\frac{k_\perp^2 + m^2}{x}\right)_i < 0 \quad . \tag{6.9}$$

The parametrization is taken to be independent of spin; the full wavefunction is then obtained by multiplying by free spinors $u/\sqrt{k^+}$. The form (6.8) has the advantage of analytic simplicity: For example, the resulting baryon distribution amplitude at small κ is

$$\phi(x_i,\kappa) = A_\phi\, x_1 x_2 x_3\, e^{-b_3^2 \sum_{i=1}^{3} \frac{m_i^2}{x_i}} \quad . \tag{6.10}$$

At large κ, ϕ is determined from the evolution equation (4.33). At very large $k_\perp$ the ψ_n for non-valence Fock states should match onto the power-law fall-off $k_\perp^{-1}$ predicted by perturbative QCD. It should be emphasized that the form (6.8) is chosen just for simplicity. An equally plausible parametrization is $\psi_n \sim A_n \mathcal{E}_n^{-p}$ with $p = 3$, which is suggested by the Schroedinger equation assuming a linear potential.

In the case of the pion we can derive two important constraints on the valence wavefunction from the $\pi \to \mu\nu$ and $\pi^0 \to \gamma\gamma$ decay amplitudes:

$$\int \frac{d^2k_\perp}{16\pi^3} \int_0^1 dx\, \psi^\kappa(x,k_\perp) = \frac{f_\pi}{2\sqrt{n_c}} \left(1 + O(\frac{m_\pi^2}{\kappa^2})\right) \tag{6.11}$$

and[27]

$$\psi^\kappa(x,k_\perp = 0)\, \frac{Z_2(m_\pi^2)}{Z_2(\kappa^2)} = \frac{\sqrt{n_c}}{f_\pi} \quad . \tag{6.12}$$

The derivation of the second constraint assumes that the radius of the pion is much smaller than its Compton length:

$$m_q^2, m_\pi^2 << 6/R_\pi^2 \quad . \tag{6.13}$$

Let us now assume the form

$$\psi^\kappa_{q\bar{q}} \propto e^{-b_V^2 (\frac{k_\perp^2 + m^2}{x(1-x)})} \quad , \qquad (\kappa^2 < 1\ \mathrm{GeV}^2) \tag{6.14}$$

where

$$-\frac{d}{dQ^2} F_\pi^V(Q^2)\Big|_{Q^2=0} = \frac{1}{6} (R_\pi^{q\bar{q}})^2 = b_V^2 \tag{6.15}$$

is the contribution to the slope of the meson form factor from the valence Fock state (see Eq. (4.2)). The two conditions (6.11) and (6.12) then determine $R_\pi^{q\bar{q}} = 0.42$ fm, and[27]

$$P^\kappa_{q\bar{q}/\pi} = \int \frac{d^2k_\perp}{16\pi^3} \int_0^1 dx \left|\psi^\kappa_{q\bar{q}/\pi}(x,\vec{k}_\perp)\right|^2 = \frac{1}{4} \left(\frac{Z_2(\kappa^2)}{Z_2(m_\pi^2)}\right)^2 \leq \frac{1}{4} \quad . \tag{6.16}$$

Thus the probability that the pion contains only the valence Fock state at small κ^2 is less than 1/4. Furthermore the radius of the valence state turns out to be smaller than that of the total state

($R_\pi^{expt} \cong 0.7$ fm). One can also verify that the bound $P_{q\bar{q}/\pi} \leq 1/4$ is also true for power-law wavefunctions $\psi \sim \xi^{-p}$, $p > 2$.

The existence of other Fock states at equal τ in the pion is to be expected considering the fact that its quark and gluon constituents are relativistic. The existence of large m_ρ/m_π and m_Δ/m_N spin splittings (due to transverse-polarized gluon exchange) also implies that there is a non-zero gluon component intrinsic to both meson and nucleon bound states.

In the case of the baryon wavefunction, one can obtain non-trivial constraints on the form of the 3-quark valence wavefunction by making a simultaneous analysis of the proton and neutron form factors and the $\psi \to p\bar{p}$ decay amplitude, assuming that the ψ decays via a 3-gluon intermediate state (see Fig. 6). The observed angular distribution[53] for $\psi \to p\bar{p}$ is in fact consistent with the predicted form $1 + \beta^2\cos^2\theta$ (where β is the nucleon velocity) and is non-trivial check of hadron helicity conservation for exclusive processes in QCD.

The $\psi \to p\bar{p}$ ratio is given to leading order in α_s by (Fig.1(b))[18]

$$\frac{\Gamma(\psi \to 3g \to p\bar{p})}{\Gamma(\psi \to 3g \to all)} = 3.2 \times 10^6 \; \alpha_s^3(s) \; \frac{|\vec{p}_{CM}|}{\sqrt{s}} \; \frac{\langle T \rangle^2}{s^4} \tag{6.17}$$

where $|\vec{p}_{CM}|/\sqrt{s} \simeq .4$, $s = 9.6$ GeV^2, and

$$\langle T \rangle \equiv \int_0^1 [dx][dy] \; \frac{\phi^*(y_i,s)}{y_1y_2y_3} \; \frac{x_1y_3 + x_3y_1}{[x_1(1-y_1) + y_1(1-x_1)][x_3(1-y_3) + y_3(1-x_3)]} \times \frac{\phi(x_i,s)}{x_1x_2x_3} \tag{6.18}$$

is a well defined function of the baryon distribution amplitude. In the case of the nuclear form factors (see Eqs. (4.6), (4.7)) it is important to use the correct argument for each α_s in the hard scattering amplitude T_H corresponding to the actual momentum transfer which flows through each exchanged gluon in Fig. 7(b). This effect is expected to yield the most important contribution to next to leading order in α_s and is an integral part of the QCD predictions. It is interesting to note that if $\phi_B = A_\phi x_1x_2x_3$ and if all the α_s have the same argument (which is in fact the situation in the asymptotic $Q^2 \to \infty$ limit[9,19]) then Eqs. (4.3)-(4.7) give

$$\lim_{Q^2 \to \infty} G_M^p(Q^2)/G_M^n(Q^2) = 0 \; .$$

However, the fact that α_s is not a constant and has different arguments for each diagram in T_1 allows one to obtain empirically consistent results for the normalization[75] of $G_M^p(Q^2)$, $G_M^n(Q^2)$ and the $\psi \to p\bar{p}$ decay rate. To first approximation one requires[27]

$$\frac{\alpha_s(x_i y_i Q^2)}{\alpha_s((1-x_i)(1-y_i)Q^2)} \cong \frac{\alpha_s(Q^2/9)}{\alpha_s(4Q^2/9)} \sim 1.5 \text{ to } 2.0 \text{ at } Q^2 \cong 10 \text{ GeV}^2 \ . \tag{6.19}$$

The QCD predictions (4.3)-(4.7) for the proton and neutron form factors are only valid at large Q^2 where the effects of mass corrections, higher Fock states and finite transverse momentum can be neglected. In order to understand these effects we extend the parametrization of the 3 quark valence Fock state contribution by using $(Q^2+M_0^2)^{-2}$ in the denominators of (4.4), (4.5) and replacing $\alpha_s(Q^2) \to \alpha_s(Q^2+M^2) = 4\pi/\beta_0 \log((Q^2+M^2)/\Lambda^2)$ to reflect the fact that at low Q^2 the transverse momenta intrinsic to the bound state wavefunctions flow through all the propagators.

Although we have not tried to optimize the parametrizations, a typical fit which is compatible with the proton and neutron form factors (see Fig. 16) and $\psi \to p\bar{p}$ decay data is $M_o \cong 1.5$ GeV, $\mu \cong 450$ MeV, $m_q \cong 300$ MeV, and $\Lambda = 280$ MeV, so that $\alpha_s(Q^2 = 10 \text{ GeV}^2) \cong 0.29$. [Analyses[50] of higher order QCD corrections to the meson form factors suggest that one can identify the Λ used here with $\Lambda_{mom} = 2.16\ \Lambda_{\overline{MS}}$.] The computed radius of the 3-quark valence state (computed from G_M via Eq. (4.2)) is however quite small: $R_V \cong 0.23$ fm, and the valence Fock state probability is $P_{qqq/p} \gtrsim 1/4$. If this

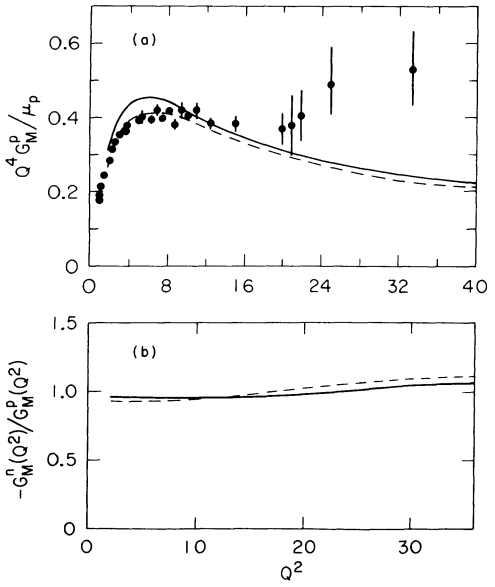

Fig. 16. Fit to nucleon form factor data described in the text. (From Ref. 27.)

preliminary analysis is correct, then, as in the meson case, the valence state is much smaller in transverse size than the physical hadron (which receives contributions to its charge radius from all Fock states).

The most crucial prediction from this analysis is that $Q^4 G_M^p(Q^2)$ should decrease by a factor of 2 for $Q^2 = 10$ to $Q^2 = 40$ GeV^2, a trend not at all indicated by the data! Further measurements of $G_M(Q^2)$ are clearly crucial in order to check this essential prediction of asymptotic freedom.

Given the above parametrization of the nucleon valence Fock state we can use Eq. (5.8) to compute the 3-quark non-perturbative contribution to the proton structure function at large x (see Fig. 17):

$$G^V_{q/p}(x,Q_o^2) \propto x(1-x)^3 \, e^{-2m^2b^2\left(\frac{1}{x}+\frac{2}{1-x}\right)} \quad . \tag{6.20}$$

Since $4m^2b^2 \sim 0.05$, the exponential factor is not very important away from the edge of phase space and so it is difficult to distinguish between the non-perturbative and $(1-x)^3$ perturbative contributions at large x (see Section V). Higher Fock states $|qqqg\rangle$, $|qqq\,\bar{q}q\rangle$ are expected to give the dominant contribution at lower x. Despite the freedom in this parametrization it is reassuring that one can simultaneously fit a number of diverse nucleon properties with QCD formulae and parameters which are the expected range.

At low Q^2 the exact formula (3.2) can be used as a further constraint on the baryon Fock states. Eventually one hopes to extend the predictions to other domains of baryon phenomenology such as the baryon decay amplitude in grand unified models and the

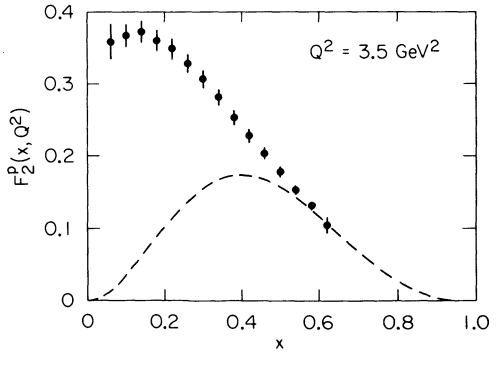

Fig. 17. Predicted valence quark contribution to the proton structure function. Evolution and higher Fock states are not included. (From Ref. 27.)

normalization of higher twist subprocesses contributions to inelastic lepton-nucleon scattering.

C. Quark Jet Diffraction Excitation[30]

The fact that the wavefunction of a hadron is a superposition of (infrared and ultraviolet finite) Fock amplitudes of fixed particle number but varying spatial and spin structure leads to the prediction of a novel effect in QCD.[30] We first note that the existence of the decay amplitude $\pi \to \mu\nu$ requires a finite probability amplitude for the pion to exist as a quark and diquark at zero transverse separation:

$$\psi(x, \vec{r}_\perp = 0) = \sqrt{4\pi}\ \sqrt{n_c}\ x(1-x) f_\pi \quad . \tag{6.21}$$

In a QCD-based picture of the total hadron-hadron cross section, the components of a color singlet wavefunction with small transverse separation interacts only weakly with the color field, and thus can pass freely through a hadronic target while the other components interact strongly. A large nuclear target will thus act as a filter removing from the beam all but the short-range components of the projectile wavefunction. The associated cross section for diffractive production of the inelastic states described by the short range components is then equal to the elastic scattering cross section of the projectile on the target multiplied by the probability that sufficiently small transverse separation configurations are present in the wavefunction. In the case of the pion interacting in a nucleus one computes the cross section

$$\frac{d\sigma}{dx\, d^2 r_\perp} \cong_{r_\perp^2 \sim 0} \sigma_{e\ell}^{\pi A}\, 12\pi\, f_\pi^2\, x^2 (1-x)^2 \tag{6.22}$$

corresponding to the production of two jets just outside the nuclear volume. The x distribution corresponds to $d\sigma/d\cos\theta \sim \sin^2\theta$ for the jet angular distribution in the $q\bar{q}$ center of mass. By taking into account the absorption of hadrons in the nucleus at $\vec{r}_\perp \neq 0$ one can also compute the $k_\perp$ distribution of the jets and the mass spectrum of the diffractive hadron system. Details are in given in Reference 30.

D. The "Unveiling" of the Hadronic Wavefunction and Intrinsic Charm

The normalizability of QCD implies that all of the dynamics of the hadron wavefunction $\psi_n^K(x_i, k_{\perp i})$ at scales κ^2 much larger than mass thresholds is completely contained in the structure of the running coupling constant $\alpha_s(\kappa^2)$ and running mass $m(\kappa^2)$ and the quark and gluon external line renormalization constants. Nevertheless, the fact that there are different hadronic scales and thresholds in QCD does imply non-trivial dynamical structure of the wavefunctions. In the case of Compton scattering, $\gamma p \to \gamma p$, the

energy denominators (see Eq. (5.3)) are a function of $2M\nu - \mathcal{E}_n$, so that the cross section is sensitive to wavefunctions up to the scale $\kappa^2 \sim 2m\nu$.

As an example of the change of wavefunction physics with the resolution scale let us consider a deuteron target. For very low $\kappa^2 << 2M\varepsilon_{B.E.}$ the deuteron acts as a coherent object. At the scale $\kappa^2 >> 2M\varepsilon_{B.E.}$, the wavefunction corresponds to a n-p bound state. As the scale increases to $\kappa^2 \lesssim 1$ GeV^2, the quark degrees of freedom become relevant and the deuteron wavefunction in QCD must be described in terms of six quark (and higher) Fock states:[76]

$$|d\rangle = a|(uud)_1(ddu)_1\rangle + b|(uud)_8(ddu)_8\rangle + c|(uuu)_1(ddd)_1\rangle + d|(uuu)_8(ddd)_8\rangle + \ldots \quad (6.23)$$

The first component corresponds to the usual n-p structure of the deuteron. The second component corresponds to "hidden color" or "color polarized" configurations where the three-quark clusters are in color-octets, but the overall state is a color-singlet. The last two components are the corresponding isobar configurations. If we suppose that at low relative momentum the deuteron is dominated by the n-p configuration, then quark-quark scattering via single gluon exchange generates the color polarized states (b) and (d) at high $k_\perp$; i.e., there must be mixing with color-polarized states in the deuteron wavefunction at short distances.[67]

The deuteron's Fock state structure is thus much richer in QCD than it is in nuclear physics where the only degrees of freedom are hadrons.

It is interesting to speculate on whether the existence of these new configurations in normal nuclei could be related to the repulsive core of the nucleon-nucleon potential,[76] and the enhancement[76] of parity-violating effects in nuclear capture reactions. One may also expect that there are resonance states with nuclear quantum numbers which are dominantly color-polarized. The mass of these states is not known. It has also been speculated[77,78] that such long-lived states could have an enormously large interaction cross section, and thus account for the Judek[79] anomaly in cosmic ray and heavy ion experiments. Independent of these speculations, it is clearly important that detailed high-resolution searches for these states be conducted, particularly in inelastic electron scattering and tagged photon nuclear target experiments, such as $\gamma d \to \gamma d$ scattering at large angles.

The structure of the photon's Fock states in QCD is evidently richer than that expected in the vector meson dominance model.[80]

For example, consider the one-gluon exchange correction to the $\gamma \to q\bar{q}$ vertex. For $\ell_\perp^2 < O(\kappa^2)$ the vertex correction renormalizes the point-vertex. For the soft domain $\ell_\perp^2 < O(\kappa^2)$ one expects large corrections which eventually by dispersion theory correspond to the usual ρ, ω, ϕ,... interpolating fields. The soft corrections thus give the usual hadron-like component of real photon interactions. Nevertheless, the point-like component survives at any momentum scale,[80] producing point-like corrections to photon shadowing, $J = 0$ fixed pole phenomena in the Compton amplitude, and the "antiscaling" QCD structure function of the photon.[13] As the resolution scale κ^2 increases past the heavy quark thresholds, one adds the $\gamma \to c\bar{c}$, $b\bar{b}$, etc. components to the photon's wavefunctions.

It is also interesting to consider the dynamical changes to the nucleon wavefunction as one passes heavy quark thresholds. For $\kappa^2 > 4m_c^2$ the proton Fock state structure contains charm quarks, e.g., states $|p\rangle \sim |uud\, c\bar{c}\rangle$. We can distinguish two types of contributions to this Fock state.[31] (1) The "extrinsic" or interaction-dependent component generated from quark self energy diagrams as shown in Fig. 18(b) — a component which evolves by the usual QCD equations with the photon mass scale Q^2; and (2) the "intrinsic" or interaction-independent component which is generated by the QCD potential and equations of motion for the proton, as in Fig. 18(a) — a component which contributes to the proton Fock state without regard to QCD evolution. Since the intrinsic component is maximal for minimum off-shell energy $\mathcal{E} = M^2 - \sum_i [(k_\perp^2 + m^2)/x]_i$ the charm quarks tend to have the largest momentum fraction x in the Fock state. (This also agrees with the physical picture that all the constituents of a bound state tend to have the same velocity in the rest frame, i.e., strong correlations in rapidity.) Thus heavy quarks (though rare) carry most of the momentum in the Fock state in which they are present — in contrast in the usual parton model assumption that non-valence sea quarks are always found at low x. One can also estimate[81] using the bag model and perturbative QCD that the probability of finding intrinsic charm in the proton is ~1-2%.

The diffraction dissociation of the proton's intrinsic charm state[31,30] provides a simple explanation why charmed baryons and charmed mesons which contain no valence quarks in common with the

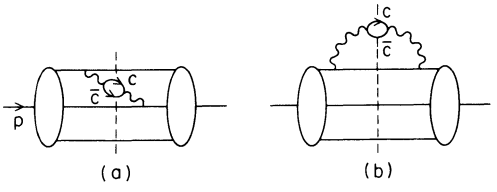

Fig. 18. Intrinsic (a) and extrinsic (b) contributions to the proton $|uud\, c\bar{c}\rangle$ Fock state.

proton are diffractively produced at large x_L with sizeable cross sections at ISR energies. Further discussion may be found in Reference 31.

VII. CONCLUSION

In these lectures we have discussed the application of QCD to hadron dynamics at short distances where asymptotic freedom allows a systematic perturbative approach. We have shown that it is possible to define the perturbative expansion in $\alpha_s(Q^2)$ in such a way as to avoid ambiguities due to choice of renormalization scheme or scale, at least in the first non-trivial orders.[14,28] Our main emphasis in these lectures, however, has been on how to systematically incorporate the effects of the hadronic wavefunction in large momentum transfer exclusive and inclusive reactions — thus leading to a broader testing ground for QCD. We have particularly emphasized the Fock state wavefunctions $\psi_n(x_i, k_{\perp i}; \lambda_i)$ which define the hadron in terms of its quark and gluon degrees of freedom at equal time on the light-cone. It is clear that a central problem of QCD is to determine not only the spectrum of the theory but also the basic bound state wavefunctions of the color singlet sector. Such solutions may be found in the near future using lattice numerical methods, particularly by quantizing at equal time on the light-cone, or by more direct attacks on the QCD equations of motion for the ψ_n, as discussed in Section III.

Even without explicit solutions for the ψ_n, we can make a number of basic and phenomenological statements concerning the form of the wavefunctions:[27]

(1) Given the ψ_n we can compute the single and multiple quark and gluon distribution amplitudes and structure functions which appear as the coefficient functions in the QCD predictions for high momentum transfer exclusive and inclusive reactions, including dynamical higher twist contributions. We have also emphasized general features of these distributions, including helicity selection rules, Lorentz properties, connections, with the Bethe-Salpeter amplitudes, renormalization properties, and correspondence limits in the non-relativistic weak binding approximation.

(2) The perturbative structure of QCD leads to predictions for the high $k_\perp$, $x \to 1$ and far-off shell behavior of the wavefunction. In particular, the large $k_\perp$ power-law behavior $\psi_V \sim k_\perp^{-2}$ of the valence wavefunctions and the $|\psi|^2 \sim k_\perp^{-2}$ behavior of the higher Fock state contributions leads to QCD evolution equations and light-cone operator product expansion for the essential measures of the wavefunctions, the distribution amplitudes $\phi_M(x,Q)$ and $\phi_B(x_i,Q)$, and the structure functions. We have also emphasized the fact that the valence wavefunction behavior $\psi_V \sim k_\perp^{-2}$ implies

that the high $k_\perp^2$ behavior of quark and gluon jet distributions $dN/dk_\perp^2$ is $\sim 1/k_\perp^4$, not exponential or gaussian.

(3) Important boundary values and constraints on hadronic wavefunctions are obtained from the weak and electromagnetic decay amplitudes, including $\psi \to B\bar{B}$. The distribution amplitudes are measurable in detail from the angular behavior of the $\gamma\gamma \to M\bar{M}$ and[82] $\gamma\gamma \to B\bar{B}$ amplitudes.

(4) By assuming simple analytic forms for the valence wavefunctions in the non-perturbative domain, we have found consistent parametrizations which are compatible with the data for hadron form factors, decay amplitudes, etc. An important feature which emerges from these studies is that the valence state is more compact in transverse dimensions than the physical hadron. Even at a low momentum transfer scale, higher Fock states play an important role, i.e., there is no scale where the proton can be identified as a 3-quark valence state. This observation may be compatible with the traditional nuclear physics picture of the nucleon as a central core, surrounded by a light-meson cloud.

(5) The fact that there is a finite probability for a hadron to exist as its valence state alone, implies the existence of a new class of "directly-coupled" semi-inclusive processes where a meson or baryon is produced singly at large transverse momentum, or interacts in a high-momentum transfer reaction without accompanying radiation or structure function evolution.[29] As in the case of directly-coupled photon reactions, the hadron can interact directly with quark and gluons in the short-distance subprocesses, with a normalization specified rigorously in terms of the distribution amplitudes or form factors. Examples of these subprocesses are $qq \to B\bar{q}$, $gq \to Mq$, $Mg \to q\bar{q}$, $B\bar{q} \to qq$. We have also discussed an important contribution to the longitudinal meson structure function $F_L^M \sim C/Q^2$, involving direct-coupling of the meson, somewhat analogous to the photon-structure function. The finite probability for a meson to exist as a $q\bar{q}$ Fock state at small separation also implies a new class of diffractive dissociation processes.[30]

(6) The Fock state description of hadrons in QCD also has interesting implications for nuclear states, especially aspects involving hidden color configurations. More generally, we have emphasized the idea that the far-off shell components of hadron wavefunctions can be "unveiled" as the energy resolution scale is increased. For example, the existence of heavy quark vacuum polarization processes within the hadronic bound state implies finite probabilities for hidden charm Fock states even in light mesons and baryons. The diffractive dissociation of these rare states appears to provide a natural explanation of the remarkable features of the charm production cross sections measured at the ISR.[31]

(7) We have also emphasized the importance of initial state interactions in all inclusive reactions involving hadron-hadron collisions. The initial state interactions disturb the color coherence, $k_\perp$ distributions, and at low energies the x-dependence of the incoming hadronic distributions. Despite these profound effects on the hadronic Fock states, some of the essential features of the QCD predictions still are retained. A detailed discussion is given in Reference 20.

Thus, in summary, we have found that the testing ground of perturbative QCD where rigorous, definitive tests of the theory can be made can now be extended throughout a large domain of large momentum transfer exclusive and inclusive lepton, photon, and hadron reactions. With the possible exception of hadron production at large transverse momentum, a consistent picture of these reactions is now emerging. By taking into account the structure of hadronic wavefunctions, we have the opportunity of greatly extending the QCD testing ground, unifying the short and long distance physics of the theory, and eventually making contact with the realm of hadronic spectroscopy, low momentum transfer reactions, and non-perturbative physics.

ACKNOWLEDGEMENT

The work was supported by the Department of Energy, contract DE-AC03-76SF00515.

REFERENCES

1. Reviews of QCD are given in: A. J. Buras, Rev. Mod. Phys. 52, 199 (1980); A. H. Mueller, Phys. Rep. 73C, 237 (1981); E. Reya, Phys. Rep. 69, 195 (1981); G. Alterelli, Univ. of Rome preprint 701 (1978); W. Marciano and H. Pagels, Phys. Rep. 36C, 137 (1978); S. J. Brodsky and G. P. Lepage, Proceedings of the SLAC Summer Inst. on Particle Physics, 1979. See also "Perturbative Quantum Chromodynamics" (Tallahassee, 1981). AIP Proceedings No. 74, New York, 1981.
2. For recent reviews of the phenomenology of QCD see A. J. Buras, FERMILAB-CONF-81/69-THY and A. H. Mueller, CU-TP-219 (1981), to be published in the Proc. of the 1981 International Symposium on Lepton and Photon Interactions at High Energies, Bonn, August 1981.
3. S. Gupta and H. R. Quinn, SLAC-PUB-2763 (1981).
4. H. D. Politzer, Phys. Rev. Lett. 30, 1346 (1973); D. J. Gross and F. Wilczek, Phys. Rev. Lett. 30, 123 (1973).
5. See, e.g., Sau Lan Wu, DESY-81-071 (1981) and Proc. of the 1981 SLAC Summer Inst. on Particle Physics. See also the 1981 Proc. of the IVth Int. Colloq. on Photon-Photon Interactions, Paris (ed. G. London).

6. TASSO Collaboration: R. Brandelik et al., DESY Report 81/053 (1981). JADE Collaboration: W. Bartel et al., DESY Report 81/048 (1981).
7. PLUTO Collaboration: see W. Wagner, Proc. of the XXth Int. Conf. on High Energy Physics, Madison, 1980; Ch. Berger et al., DESY preprint 81/051 (1981).
8. S. J. Brodsky and G. R. Farrar, Phys. Rev. Lett. 31, 1153 (1973) and Phys. Rev. D11, 1309 (1975); V. A. Matveev, R. M. Muradyan and A. V. Tavkheldize, Lett. Nuovo Cimento 7, 719 (1973).
9. S. J. Brodsky and G. P. Lepage, Phys. Rev. Lett. 43, 545, 1625(E) (1979); S. J. Brodsky, G. P. Lepage and S. A. A. Zaidi, Phys. Rev. D23, 1152 (1981).
10. For a review of high momentum transfer exclusive processes and references, see A. H. Mueller, Ref. 1.
11. S. J. Brodsky and G. P. Lepage, SLAC-PUB-2294, published in "Quantum Chromodynamics," Wm. Frazer and F. Henyey (eds.) (AIP, 1979), Phys. Lett. 87B, 359 (1979), S. J. Brodsky, Y. Frishman, G. P. Lepage and C. Sachrajda, Phys. Lett. 91B, 239 (1980). See also A. V. Efremov and A. V. Radyushkin, Rev. Nuovo Cimento 3, 1 (1980); Phys. Lett. 94B, 245 (1980). A. Duncan and A. Mueller, Phys. Rev. D21, 1636 (1980); Phys. Lett. 90B, 159 (1980). G. R. Farrar and D. R. Jackson, Phys. Rev. Lett. 43, 246 (1979); V. L. Chernyak and A. R. Vhitnishii, JETP Lett. 25, 11 (1977); G. Parisi, Phys. Lett. 43, 246 (1979); M. K. Chase, Nucl. Phys. B167, 125 (1980).
12. S. J. Brodsky and G. P. Lepage, Phys. Rev. D24, 1808 (1981).
13. E. Witten, Nucl. Phys. B120, 189 (1977); V. A. Bardeen and A. J. Buras, Phys. Rev. D20, 166 (1979).
14. S. J. Brodsky, G. P. Lepage, P. B. Mackenzie (to be published).
15. For early work on higher twist contributions see: R. Blankenbecler, S. J. Brodsky and J. F. Gunion, Phys. Rev. D18, 900 (1978); and D. Sivers, S. J. Brodsky and R. Blankenbecler, Phys. Rep. 23C, 1 (1976) and references therein. Higher twist contributions to deep inelastic scattering were first discussed in detail by: R. Blankenbecler and I. A. Schmidt, Phys. Rev. D16, 1318 (1977); L. F. Abbott and R. M. Barnett, Annals Phys. 125, 276 (1980); G. R. Farrar and D. R. Jackson, Phys. Rev. Lett. 35, 1416 (1975). See also L. F. Abbott, E. L. Berger, R. Blankenbecler and G. Kane, Phys. Lett. 88B, 157 (1979); L. F. Abbott, W. B. Atwood and R. M. Barnett, Phys. Rev. D22, 582 (1980), and references therein. More general frameworks for dynamical higher twist contributions are given in W. E. Caswell, R. R. Horgan and S. J. Brodsky, Phys. Rev. D18, 2415 (1978); and H. D. Politzer, Nucl. Phys. B172, 349 (1980); and S. J. Brodsky and G. P. Lepage, Ref. 1. Specific QCD calculations are given in G. R. Farrar and G. C. Fox, Nucl. Phys. B167, 205 (1980); E. L. Berger, T. Gottschalk and D. Sivers, Phys. Rev. D23, 99 (1981); E. L. Berger and S. J. Brodsky, Phys. Rev. Lett. 42, 940 (1979), Phys. Rev. D24, 2428 (1981); E. L. Berger, Phys. Lett. 89B, 241 (1980); R. L. Jaffe and M. Soldate, Phys. Lett. 105B, 467 (1981).

16. For a review of experimental evidence on higher twist terms in deep inelastic scattering see C. Matteuzzi, SLAC-PUB-2827 (1981).
17. P. V. Landshoff, Phys. Rev. D10, 1024 (1974); P. Cvitanovic, Phys. Rev. D10, 338 (1974); S. J. Brodsky and G. Farrar, Phys. Rev. D11, 1309 (1975).
18. S. J. Brodsky and G. P. Lepage, SLAC-PUB-2746 (1981), to be published in Phys. Rev.
19. G. P. Lepage and S. J. Brodsky, Phys. Rev. D22, 2157 (1980).
20. G. T. Bodwin, S. J. Brodsky and G. P. Lepage, Phys. Rev. Lett. 47, 1799 (1981); G. T. Bodwin (this volume).
21. S. J. Brodsky and G. P. Lepage, Ref. 1; and S. J. Brodsky and G. P. Lepage, SLAC-PUB-2601 (1980), presented at the XXth Int. Conf. on High Energy Physics, Madison, Wisc. (1980).
22. G. R. Farrar and D. R. Jackson, Ref. 15; D. L. Berger and S. J. Brodsky, Ref. 15.
23. For an early discussion see T. A. DeGrand, Y. J. Ng and S. H. H. Tye, Phys. Rev. D16, 3251 (1977). The large $k_\perp$ behavior of hadronic wavefunctions in QCD is discussed by S. J. Brodsky, Y. Frishman, G. P. Lepage and C. Sachrajda, Ref. 11. See also S. J. Brodsky and G. P. Lepage, Ref. 1. These contributions are in principle normalizable in QCD using the methods of Ref. 19.
24. E. L. Berger, T. Gottschalk and D. Sivers, Ref. 15. G. Farrar and G. Fox, Ref. 15.
25. G. Parisi, Phys. Lett. 43, 246 (1978). A. Duncan and A. H. Mueller, Ref. 11.
26. See, e.g., S. J. Brodsky, F. E. Close, J. F. Gunion, Phys. Rev. D6, 177 (1972). G. Grammer and J. Sullivan, in Electrons in the Interactions of Hadrons (eds. A. Donaghue and G. Shaw), Plenum Press (1977). T. H. Bauer, R. D. Spital, D. R. Yennie and F. M. Pipkin, Rev. Mod. Phys. 50, 261 (1978).
27. S. J. Brodsky, T. Huang, G. P. Lepage, SLAC-PUB-2540 (1980), and T. Huang, SLAC-PUB-2580 (1980), published in the Proceedings of the XXth Int. Conf. on High Energy Physics, Madison, Wisc. (1980). The parametrization of the hadronic wavefunctions presented here are preliminary; a complete discussion and final values will be given by S. J. Brodsky, T. Huang and G. P. Lepage (in preparation).
28. A more detailed discussion of the regularization procedure is given by G. P. Lepage, presented at the Banff Summer Institute on Particle Physics (1981) (this volume).
29. E. L. Berger and S. J. Brodsky, Phys. Rev. D24, 2428 (1981).
30. G. Bertsch, S. J. Brodsky, A. S. Goldhaber and J. G. Gunion, Phys. Rev. Lett. 47, 297 (1981)
31. S. J. Brodsky, P. Hoyer, C. Peterson and N. Sakai, Phys. Lett. 93B, 451 (1980).
32. S. J. Brodsky, C. Peterson and N. Sakai, Phys. Rev. D23, 2745 (1981).
33. C. Peterson, SLAC-PUB-2775 (1981).

34. See, e.g. K. Callan, R. Dashen and D. Gross, "Quantum Chromodynamics," Proceedings of the 1978 La Jolla Summer Institute, Wm. Frazer and F. Henyey (eds.), AIP (1979).
35. For reviews and references for inclusive process factorization see A. J. Buras, Ref. 1. For exclusive processes see Ref. 19 and A. H. Mueller, Ref. 1.
36. M. Creutz, in "Perturbative Quantum Chromodynamics" AIP Conference Proceedings #74 (1981), and this volume.
37. H. R. Quinn and M. Weinstein, SLAC-PUB-2795 (1981), and references therein. D. Horn and M. Weinstein, SLAC-PUB-2864 (1981).
38. R. Blankenbecler, D. J. Scalapino and R. L. Sugar, Phys. Rev. D24, 2778 (1981); J. E. Hirsh, D. J. Scalapino, R. L. Sugar and R. Blankenbecler, NSF-ITP-81-89 (1981).
39. For a recent review of Bag models see L. Heller, Los Alamos preprint LA-UR-81-3026.
40. S. J. Brodsky and G. P. Lepage, Ref. 1.
41. See Refs. 27 and 29; G. P. Lepage and P. B. MacKenzie, Cornell preprint CLNS/81-498 (1981).
42. P. A. M. Dirac, Rev. Mod. Phys. 21, 392 (1949).
43. S. Weinberg, Phys. Rev. 150, 1313 (1966); L. Susskind and G. Frye, Phys. Rev. 165, 1535 (1968); J. B. Kogut and D. E. Soper, Phys. Rev. D1, 2901 (1970); J. D. Bjorken, J. B. Kogut and D. E. Soper, Phys. Rev. D3, 1382 (1971); S. J. Brodsky, R. Roskies and R. Suaya, Phys. Rev. D8, 4574 (1973).
44. J. D. Bjorken et al., Ref. 43.
45. The regularization can be performed using Pauli-Villars regularization. See Ref. 28.
46. S. D. Drell and T. M. Yan, Phys. Rev. Lett. 24, 181 (1970).
47. S. J. Brodsky and S. D. Drell, Phys. Rev. D22, 2236 (1981).
48. S. J. Brodsky and T. Huang (in preparation).
49. S. J. Brodsky, Y. Frishman, G. P. Lepage and C. Sachrajda, Ref. 11.
50. R. D. Field, R. Gupta, S. Otto and L. Chang, Nucl. Phys. B186, 429 (1981); F. M. Dittes and A. V. Radyushkin, Dubna preprint JINR-E2-80-688 (1980); M. Chase, Ref. 11; E. Braaten (private communication).
51. G. R. Farrar and D. R. Jackson, Phys. Rev. Lett. 43, 246 (1979).
52. M. Peskin, Phys. Lett. 88B, 128 (1979).
53. A. Duncan and A. Mueller, Phys. Rev. D21, 636 (1980); Phys. Lett. 98B, 159 (1980); A. Mueller, Ref. 1.
54. S. J. Brodsky, G. P. Lepage and S. A. A. Zaidi, Phys. Rev. D23, 1152 (1981).
55. I. Peruzzi et al., Phys. Rev. D17, 2901 (1978).
56. See, e.g. S. J. Brodsky, F. E. Close and J. F. Gunion, Phys. Rev. D5, 1384 (1972); D8, 3678 (1973).
57. J. D. Bjorken, Phys. Rev. 163, 1767 (1967); 179, 1547 (1969).
58. G. Alterelli and G. Parisi, Nucl. Phys. B126, 298 (1977). See also, V. N. Gribov and L. N. Lipatov, Sov. J. Nucl. Phys. 15, 483, 675 (1972); J. Kogut and L. Susskind, Phys. Rev. D9, 697, 706, 3391

(1974); L. N. Lipatov, Sov. J. Nucl. Phys. 20, 94 (1975).
59. R. D. Field published in "Quantum Chromodynamics," Wm. Frazer and F. Henyey (eds.) AIP (1979).
60. R. Blankenbecler and S. J. Brodsky, Phys. Rev. D10, 2973 (1974).
61. F. Martin and A. DeRujula, Phys. Rev. D22, 1787 (1980).
62. G. R. Farrar and D. R. Jackson, Phys. Rev. Lett. 35, 1416 (1975); A. I. Vainshtein and V. I. Zakharov, Phys. Lett. 72B, 368 (1978).
63. Z. F. Ezawa, Nuovo Cimento 23A, 271 (1974).
64. See also A. Duncan and A. Mueller, Ref. 54.
65. K. J. Anderson et al., Phys. Rev. Lett. 43, 1219 (1979).
66. M. Haguenauer et al., Phys. Lett. 100B, 185 (1981).
67. S. J. Brodsky and G. P. Lepage, Proceedings of the Eugene Few Body Conference 1980: 247C (Nucl. Phys. A353, 1981).
68. S. Gupta, Phys. Rev. D24, 1169 (1981).
69. See references 21, 24, 15, and S. J. Brodsky, J. F. Gunion and R. Rückl, Phys. Rev. D18, 2469 (1978). J. Bagger and J. F. Gunion, U. C. Davis preprint 81/3 (1981).
70. E. L. Berger and S. J. Brodsky, Phys. Rev. D24, 2428 (1981).
71. S. D. Ellis, P. V. Landshoff and M. Jacob, Nucl. Phys. B108, 93 (1978); P. V. Landshoff and M. Jacob, Nucl. Phys. B113, 395 (1976).
72. S. J. Brodsky, J. F. Gunion and R. Rückl, Ref. 69.
73. S. J. Brodsky, T. DeGrand, J. F. Gunion and J. Weis, Phys. Rev. D19, 1418 (1979), Phys. Rev. Lett. 41, 672 (1978); Ch. Llewellyn-Smith, Phys. Lett. 79B, 83 (1978); S. M. Berman, J. D. Bjorken and J. B. Kogut, Phys. Rev. D4, 3378 (1971).
74. W. Ochs and L. Stodolsky (private communication).
75. A review of the form factor data is given by B. T. Chertok, CERN preprint PRINT-81-0318, to be published in the Proceedings of the 16th Recontre de Moriond (1981).
76. See Ref. 67 and references therein; S. J. Brodsky, SLAC-PUB-1497 (1974) published in the Proceedings of the Int. Conf. on Few Body Problems in Nuclear and Particle Physics, University of Laval, Quebec (1974), p. 676-690, Eds. R. J. Slovodrian, B. Cujec and K. Ramavataram, Les Presses de L'université Laval (1975).
77. A. P. Kobushkin, Yad. Fiz 28, 495 (1978).
78. Y. M. Dubovik and A. P. Kobushkin, Kiev preprint ITF-78-85E (1978).
79. B. Judek, Can. J. Phys. 46, 343 (1968), Proceedings of the 14th Int. Cosmic Ray Conf., Vol. 79, p. 2343. F.M. Friedlander et al., LBL preprint 11136 (1980). Y. J. Karant, LBL preprint 9171 (1979). W. J. Romo and P. J. S. Watson, Phys. Lett. 88B, 354 (1979).
80. See, e. g., S.J. Brodsky, SLAC-PUB-2747 (1981) and W. R. Frazer, UCSD 10P10-222 (1981), published in the Proceedings of the 4th Int. Colloq. on Photon-Photon Interactions, University of Paris, 1981, and W. A. Bardeen, to be published in the Proceedings of the 1981 Int. Symp. on Lepton and Photon

Interactions at High Energies, Bonn, August 1981.
81. J. F. Donoghue and E. Golowich, Phys. Rev. D15, 3421 (1977).
82. P. Damgaard, Cornell preprint CLNS-81/519 (1981).